DESIGN OF A NOVEL THERMO-ELECTRIC COOLING DEVICE CAPABLE OF ACHIEVING CRYOGENIC TEMPERATURES FOR DENTAL PULP TESTING

A Thesis Submitted to the College of Graduate and Postdoctoral Studies

In Partial Fulfillment of the Requirements

For the Degree of Master of Science

In the Department of Mechanical Engineering

University of Saskatchewan

Saskatoon

By

BILAL MUSTAFA

Permission to Use

In presenting this thesis in partial fulfillment of the requirements for a Master of Science degree from the University of Saskatchewan, I agree that the Libraries of this University may make it freely available for inspection. I further agree that permission for copying of this thesis in any manner, in whole or in part, for scholarly purposes may be granted by the professor or professors who supervised my thesis work or, in their absence, by the Head of the Department or the Dean of the College in which my thesis work was done. It is understood that any copying or publication or use of this thesis or parts thereof for financial gain shall not be allowed without my written permission. It is also understood that due recognition shall be given to me and to the University of Saskatchewan in any scholarly use which may be made of any material in my thesis.

Requests for permission to copy or to make other uses of materials in this thesis in whole or part should be addressed to:

Head of the Department of Mechanical Engineering
Engineering Building, University of Saskatchewan
57 Campus Drive, Saskatoon, SK, CANADA S7N 5A9

OR

College of Graduate and Postdoctoral Studies
Room 116, Thorvaldson Building, University of Saskatchewan
110 Science Place, Saskatoon, SK, CANADA S7N 5C9

Acknowledgments

Firstly, I would like to pay my respects to my supervisors, Professor W.J. (Chris) Zhang and Professor Dean Kolbinson for their unconditional support and technical guidance throughout my studies. No words are enough to express the gratitude that I have for them. Secondly, I would like to thank my committee members Professor David A. Torvi and Professor Assem Hedayat for their valuable suggestions and time. This would never have been possible without the support of all of you.

I would like to thank Doug Bitner, departmental assistant, for helping me in the lab and my former research group member Bing Zhang for his help. I would also like to thank the College of Dentistry and Saskatchewan Government for funding my studies through the Saskatchewan Innovation and Opportunity Scholarship.

In the end, I would like to thank my family and especially my mother who was always there for my moral support and always motivated me in tough times.

Abstract

Dental pulp testing is a diagnostic test in endodontics to test whether the dental pulp is dead or alive. Thermal tests (cold and hot) and electrical pulp testing techniques are two of the most common pulp sensibility tests currently being used. Although cold tests have shown more promising results in comparison to other techniques, the current methods used for cold testing have safety concerns as they involve direct application of the cold agent to the tooth. This study proposed a thermoelectric cooling based dental pulp testing device capable of achieving cryogenic temperatures and varying this temperature below 0℃ up to -60℃. This device is safe in operation and provides availability for on-site application due to its portability and stand-alone features. Thermoelectric cooling is based on the Peltier effect, which allows a temperature difference across a thermoelectric module and results in one side of the module becoming cold while the other side becomes hot. The challenge for such devices based on the Peltier effect is that the heat on the hot side of the module needs to be dissipated so that it is not too hot to burn the patient's skin. This study explored the application of the phase change cooling technique in the form of heat pipes and vapor chambers to address this challenge. Finally, a thermoelectric cooling system capable of achieving -60℃ at the probe for pulp sensibility testing was proposed through modeling and simulation in Comsol Multiphysics software and experimentally validated using off-the-shelf hardware.

Table of Contents

List of Figures

List of Tables

Nomenclature

Symbols

A	cross-sectional area, mm^2
Cp	specific heat at constant pressure, kJ/kg·K
I	electric current, A
J	current density, A/m2
k	thermal conductivity, W m^{-1} K^{-1}
K	thermal conductance, W K^{-1}
l	length of thermoelement, mm
n	normal vector to the interface
N	number of thermocouples
$\dot{Q}$	Peltier heat, watts
Q_c	Heat removed from cold side, watts
Q_h	Heat rejected at hot side, watts
R	Resistance, Ω
T_h	Temperature of the hot side, ℃
T_c	Temperature of the cold side, ℃
u	velocity vector, m/s
V	Potential Difference, volts
$\dot{W}$	Input electrical power, watts
Z	figure of merit

Greek symbols

α	Seebeck coefficient, V K^{-1}
∇	Del operator
Π	Peltier Coefficient, V
ΔT	temperature difference between hot

and cold sides, K

ρ	electrical resistivity, Ωm
τ	Thomson coefficient, V K^{-1}

Abbreviations

COP	coefficient of performance
DDM	dichlorodifluoromethane
EPT	electric pulp testing
FN	false negative
FP	false positive
IR	infrared
MEMS	micro-electrical mechanical system
PCR	polymerized chain reaction
TN	true negative
TP	true positive
TEC	thermoelectrical cooler

Subscripts

c	cold side
e	thermoelement
h	hot side
m	mean/average
max	maximum
n	n-type thermoelement
p	p-type thermoelement

Chapter 1

Introduction

1.1. Background

In the last two decades, the field of medical equipment has seen a great number of innovative solutions to improve the diagnosis and treatment of diseases. While the focus was on achieving efficiency and reliability of results, safety and portability of these instruments were also considered. However, it is difficult to accomplish both tasks, safety and portability, at the same time, and there is a limit up to which the sizes of the instruments can be reduced without disturbing the efficiency and utility of the equipment.

Dental pulp testing is an investigation frequently performed by dental clinicians, and the objective is to assess pulp health and test whether it is dead or alive. Thermal tests (cold and hot) and electrical pulp testing techniques are being currently used, and cold tests have shown more promising results in comparison to other techniques (Chen and Abbott, 2009). In cold testing, a temperature below 0℃ is applied to the tooth surface. Only if the pulp is alive, the patient will feel the temperature. There is not a set limit to the low temperature to which the person may respond, so the dentist will have to apply a range of temperatures.

1.2. Motivation

The current methods used for cold testing do not provide the dentist with an ability to apply a range of temperatures below 0℃. They also have safety concerns as they involve direct application of the cold agent to the tooth. Therefore, research is needed for an improved method along with a device for cold testing of the dental pulp (or dental pulp testing for short). This new method along with the device should answer the following questions:

Question 1: Will the proposed method ensure the safety of the patient during diagnosis?

Patient safety is always a fundamental concern to any method as well as device.

Question 2: Will the proposed method enable the dentist to apply a range of cold temperatures?

The significance of the answer to this question was discussed in section 1.1 above.

Question 3: Will the proposed method be portable and stand-alone for on-site diagnosis?

It is noted that the thermoelectric cooling technique was particularly explored in this thesis, because it is known that this technique is promising to achieve cryogenic temperatures in a small solid-state module.

1.3. Objectives

In the light of above discussion, the overall objective of this thesis was to achieve thermoelectric cooling along with a device capable of achieving cryogenic temperatures for dental pulp testing. The requirements for the device are summarized as follows (Suh, 1990; Fan et al., 2015):

Function (along with performance) requirements:

- FR1= able to generate the cryogenic temperature up to -60℃ below 0℃, decided based on the reported lowest temperature (-56℃ for CO_2 snow) for dental pulp testing in literature (Chen and Abbott, 2009).
- FR2= able to dissipate the heat at the hot side of the thermoelectric cooler such that the temperature at the hot side is below 45℃ as any temperature above this for more than 7 minutes will burn the human tissues (Yarmolenko et al., 2011).
- FR3= able to vary the temperature as desired during the dental pulp testing.
- FR4= able to maintain the desired temperature for a particular duration.

Constraint (both 'must-be' and desired) requirements:

- CR1= be small in size such that it can be held by one hand.
- CR2= be light in weight such that it can be held by one hand.
- CR3= be stand-alone and portable.

There are three specific objectives, expected to achieve the overall objective (along with the device to meet the aforementioned requirements).

Specific Objective 1: *To verify the feasibility of the thermoelectric cooling principle of the device to achieve the requirements for dental pulp testing*.

Specific Objective 2: *To develop a simulation system for the device for dental pulp testing*. The simulation system is needed to optimize the design of the device.

Specific Objective 3: *To construct a proof-of-concept prototype of the device for dental pulp testing.* The prototype is needed to test the proposed device against the requirement of the device.

1.4. Research Methodology

Commercially available thermoelectric coolers were tested with phase change heatsinks consisting of heat pipes and vapor chambers to demonstrate the ability of thermoelectric coolers to achieve -60℃. After witnessing the promising results, the device was modeled in Comsol Multiphysics to propose a thermoelectric cooling system for a dental pulp testing device that can achieve the research objectives above.

1.5. Organization of the thesis

Following chapter 1 or the introduction, chapter 2 introduces the significance of dental pulp testing as a diagnostic aid in dentistry and gives a brief introduction and comparison of various diagnostic methods currently available for this purpose. Chapter 3 provides a brief review of the concept of thermoelectric cooling, important equations, and performance parameters of a thermoelectric module. Chapter 4 will review the literature on the application of thermoelectric cooling in medical devices, focusing mainly on previous research on thermoelectric-cooling-based pulp testing. Chapter 5 will provide a brief introduction of heat dissipation methods available for a thermoelectric cooling system with a focus on phase change cooling methods like heat pipes and vapor chambers. Chapter 6 will introduce the research methodology, scope of the study and experimental work. In chapter 7, Comsol Multiphysics is utilized to model a thermoelectric cooling system for the dental pulp testing device, and off-the-shelf hardware is used to validate the design experimentally. Chapter 8 concludes the thesis.

Chapter 2

Dental Pulp Testing

2.1. Dental Pulp

The dental pulp, also known as tooth pulp or tooth nerve, is a vital part of the tooth and makes up the center of the tooth from its canals to just below the tip underneath the enamel layer and the dentin layer. It consists of connective tissues, blood vessels, nerves and cells called odontoblasts.

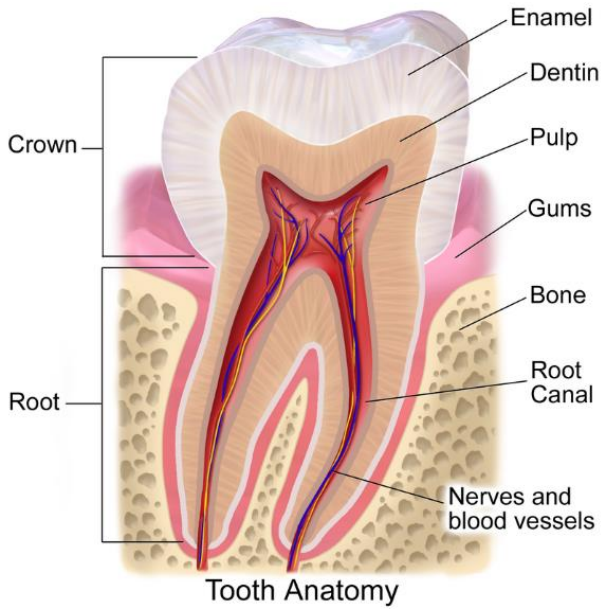

Figure 2-1. Tooth Anatomy (Blausen.com staff, 2014). Reproduced from open access journal

2.1.1. Functions of Dental Pulp

The primary function of the pulp is to form the dentin, but it has other important functions as well which include:

Sensory Function: The reason pain is felt after trauma to the dentin and/or pulp, and the sense of differences in temperature and pressures, is possible due to the stimulation of the pulp.

Formation of Dentin: In response to trauma which results in damaging the dentin layer, the pulp is capable of forming secondary dentin, also known as reparative dentin.

Nourishment: The blood vessels in the pulp keep the tooth moisturized and hence prevent it from becoming brittle (Watson, n.d.).

2.2. Damaging of Dental Pulp

While poor dental hygiene is the main reason that leads to pulpal damage, it is not the only reason. Some important causes of pulpal damage are listed below:

1. Due to poor dental hygiene, plaque can develop and lead to cavities, and if not treated promptly, it can eventually affect the pulp by penetrating through the enamel and then the dentin.
2. Physical trauma resulting in a chipped or broken tooth may expose the pulp and end up damaging it.
3. A slowly dying tooth, either due to aging or after the trauma that was left untreated at the time of injury, may infect the pulp eventually.

2.3. Pulp Diseases

Napeñas (2013) reviewed that pulp damage may result in several kinds of pulp diseases.

Reversible pulpitis: It is the mild inflammation of the pulp. Symptoms typically include pain upon eating or drinking something very sweet, hot, or cold. Without treatment, the inflammation can progress to a dental abscess, a collection of bacteria and pus. Good oral health habits can help offset reversible pulpitis, but in many cases, a filling is eventually needed.

Irreversible pulpitis: It is the severe inflammation of the pulp that cannot be cured. Symptoms include sudden intense pain. If left untreated, it can result in widespread gum and connective tissue infection. Irreversible pulpitis is generally treated with a root canal procedure. If that does not work, a dentist may have to remove the tooth.

Dental pulp exposure: This condition comes on when damage to the external covering of a tooth, such as a cavity or crack in the tooth, exposes the normally protected pulp to bacteria and irritating food particles. Pain is the most frequent symptom, and without proper dental care, a mild infection can progress into a serious abscess. Depending on the degree of pulp exposure, a filling, root-canal procedure, or even tooth extraction may be required.

2.4. Diagnosis of Dental Pulp Infection

As can be seen from the previous discussion that the dental pulp plays an important role in the tooth health and avoiding the permanent loss of a tooth, any of the pulp diseases that have the potential to exist need to be diagnosed at early stages. The most accurate way of investigating pulp health could be the histological examination of a tissue specimen from the pulp, but it is both impractical and unfeasible in the real world which leads clinicians to perform dental pulp testing to provide additional information before starting treatment. A number of tests are available at a dentist's disposal which are categorized into pulp vitality tests and pulp sensibility tests.

Pulp Vitality Tests: These tests are performed to determine the blood supply to the pulp. Pulp tissues may have an adequate blood supply, but it is not necessary that a test would stimulate them. Consequently, a tooth under observation may not respond to an external stimulus for a period following an injury as shown by clinical examinations (Chen and Abbott, 2009).

Pulp Sensibility Tests: These tests are performed to assess the pulp sensory response where sensibility is the ability to respond to a stimulus. Teeth with pulpitis are more responsive to an external stimulus as compared to the rest of the teeth and hence these tests which are cold, hot and electrical in their nature, can be used to determine pulp health. These results are then extrapolated to determine whether the pulp is healthy or inflamed depending upon how early and with what intensity the patient feels the pain. As a result of a sensibility test, three kinds of responses are possible:

(1) The response is not exaggerated, and pain does not linger, the pulp is in its normal healthy condition.
(2) There is no response at all; the pulp is deemed non-vital or dead.
(3) The response is pronounced or exaggerated, the pulp is inflamed, or pulpitis is present.

2.4.1. Pulp Sensory Response Mechanism

The pain response to a stimulus can be because of fluid movement along with other factors through the dentinal tubules (Pierce, 1998). The myelinated Aδ-fibers are afferent nerve fibers of a nociceptor and are known to have high conduction velocity due to a thin covering of myelin.

They are responsible for the sudden sharp pain whereas the unmyelinated C-fibers (smaller than Aδ-fibers) are thought to be responsible for the lingering "burning" pain (Milner et al., 2015).

2.5. Diagnostic Techniques for Pulp Sensibility

There are two major techniques for the assessment of a pulp's sensory response, thermal and electric. Thermal tests are further divided into hot and cold tests.

2.5.1. Thermal Tests

Stimulating the pulp through the application of hot or cold temperatures to the tooth surface are the most widely used pulp testing techniques. The usefulness of these techniques in diagnosis is undeniable.

Cold Test: Cold testing involves the application of any of the following cold materials to the tooth surface: ice, ethyl chloride, CO_2 snow, and dichlorodifluoromethane (DDM).

Ice: Though the simplest of all cold testing agents, ice is difficult to handle along with associated infection control issues, and direct application of ice can be problematic. Rubber dams are used to isolate the tooth from the rest of the teeth (Chen and Abbott, 2009).

Refrigerant Spray: Easy to store, low cost and simple to apply, refrigerant sprays have been widely used for pulp testing. With new refrigerants replacing old ones which were either ineffective or environmentally non-friendly, these agents are applied either using a cotton pellet, cotton bud or a cotton roll. A larger surface area of the cotton pellet is better than a smaller pellet, and a cotton bud should be preferred over a cotton roll as the roll will draw refrigerant away due to its dry fibers acting as a wick (Chen and Abbott, 2009).

Carbon Dioxide Snow (CO_2): Also known as dry ice, CO_2 snow is prepared in the form of sticks from pressurized liquid CO_2. Chen and Abbott (2009) reviewed that of all the clinical cold agents available dry ice has the lowest achievable temperature, i.e., -56℃.

Safety Concerns of Cold Tests: Concerns have been raised about potential safety hazards associated with cold tests for pulp testing, especially the use of CO_2 for the lowest clinical temperature of -56℃. Ehrmann (1977) explained the phenomenon of Leidenfrost and stated that despite a small amount of CO_2 entering the oral cavity, no harm is caused because of the formation

of CO_2 gas that surrounds the melting mass of dry ice and provides no time for soft tissue burns to occur.

Heat Test: A compound material is heated to reach its melting point and then applied on to the tooth surface directly with a lubricant which facilitates in material removal later. *Gutta-percha* is the most widely used material for the heat test for pulp testing.

Safety Concerns of Heat Tests: Chen and Abbott (2009) reviewed that the temperature of gutta-percha is 78℃ and can be up to 150℃ in the literature. Zach (1972) noted that an increase of 11℃ could harm the pulp. The *in vitro* portion of the study conducted by Fuss et al. (1998) showed that an application time of fewer than five seconds increases the pulp temperature by 2℃ which is unlikely to damage the pulp.

2.5.2. Electric Pulp Test

After thermal tests, electric pulp testing or EPT is another technique used as a pulp sensibility test. The electrical current is passed through the enamel to the pulp stimulating an ionic change across the neural membrane. The "circuit" needs to be completed by having the patient hold the test probe handle (Chen and Abbott, 2009).

Safety Concern of EPT: The major safety concern associated with EPT is the interference with a cardiac pacemaker.

2.6. Comparison of Thermal (Heat and Cold) and EPT

Petersson et al. (1998) conducted a comparative study of pulp sensibility tests using *gutta-percha*, ethyl chloride for cold testing and electrical pulp testing. The study was conducted with 65 patients with ages ranging from 21 to 79 years and responses were observed from 75 anterior and posterior teeth with healthy and diseased pulps. Relevant sensitivity, specificity, positive predictive value, negative predictive value, and accuracy for each test was evaluated with a given disease. The physical meanings of these measured values are as follows (Chen and Abbot, 2009):

True/False Negatives and Positives: Denoted as (TN, FN, TP, FP), a negative result indicates the absence of disease and positive means the presence of disease.

Sensitivity: The ability of a test to identify teeth with no pulp or with a diseased pulp is defined as sensitivity.

Sensitivity = TP/(TP + FN)

Specificity: It is the ability of a pulp test to identify pulps without the disease.

Specificity = TN/(TN + FP)

Positive Predictive Value: It is the probability that if the result is a "positive," it truly represents a tooth with a diseased pulp or with no pulp.

Positive predictive value = TP/(TP + FP)

Negative Predictive Value: It is the probability that if the result is "negative," it truly represents a disease-free pulp.

Negative predictive value = TN/(TN + FN)

Accuracy: It is the overall rate of agreement of the test results to the actual pulp health.

Accuracy = (TP + TN)/(TP + TN + FP + FN)

The results of the tests from Petersson et al. (1998) are summarized in Table 2-1.

TABLE 2-1. Comparison of pulp sensibility tests (Petersson et al., 1998)

	Cold Testing (Ethyl Chloride)	Heated *gutta-percha*	Electric Pulp Testing (EPT)
Sensitivity	.83	.86	.72
Specificity	.93	.41	.93
Positive Predictive Value	.89	.48	.88
Negative Predictive Value	.90	.83	.84
Accuracy	.86	.71	.81

The results show that cold tests are more likely to give realistic measurements of the response as compared to the other two techniques and heated *gutta-percha* gave a higher number of false positives. Jespersen et al. (2014) also concluded that patients with age ranging from 21 to 50 years gave a more reliable response to cold tests. Yu et al. (2009) cited that for EPT, false results are quite possible for a recently traumatized tooth that will not respond to the device due to a temporary loss of sensory function which leads to a false negative result. Another reason that leads to false results as reviewed by Chen and Abbott (2009) is the conduction of current to adjacent teeth due

to the presence of metallic restorations. Correct placement of the EPT probe tip flat against the contact area is another important factor that contributes to the results. Mumford (1964) compared heat and cold pulp sensibility tests using ethyl chloride and heated gutta percha on anterior teeth and premolars and noted that both ethyl chloride and heated gutta-percha failed to respond for premolar teeth, especially in adults, and cold testing was found to be more accurate than heat in the same experiment. Dummer et al. (1980) also found that in teeth diagnosed with irreversible pulpitis, heated *gutta-percha* was no more effective than ethyl chloride.

2.7. Effect of Cold Tests

Chen and Abbott (2009) cited that cracks may be formed on enamel surfaces from direct dry ice contact. To address this issue, Peters et al. (1986) conducted a three-part series of studies which included both the *in vitro* and *in vivo* effects of exposure to low temperatures. Chen and Abbott (2009) reviewed Fuss et al. (1988) who also conducted combined *in vivo* and *in vitro* studies placing CO_2 snow on teeth scheduled for extraction. These studies concluded that after five seconds of application, CO_2 snow only decreased the pulp temperature by less than 2^oC. This degree of temperature change cannot damage the pulp as pulp tissue is only irreversibly damaged after being frozen at approximately −9℃ (Frank et al., 1972). In light of these studies, it can be said that cold tests are more accurate and sensitive and that the pulp is not damaged up to the reported dry ice temperature of -52℃.

2.7.1. Limitations of Cold Tests for Pulp Sensibility and Need for Improved Safety

Though cold tests are the most efficient; there are some limitations associated with the current methods, as Chen and Abbott (2009) reviewed that cold testing can give false results as well. This is mainly attributed to teeth restored with metal crowns where cold temperatures may stimulate either the gingivae or the adjacent teeth. These restored teeth may give accurate results for a slightly higher temperature if clinicians have control over varying the applied temperature which is not possible with the current cold testing techniques being used. In addition, the current application methods have a potential safety hazard associated with them as they involve the direct application of cold agents. Considering the preceding discussion, it can be said that the need for a new cold testing technique which can provide a range of cold temperatures and is safer for the well-being of patients is inevitable.

Chapter 3

Introduction to Thermoelectric Cooling

3.1. Thermoelectric Effect

The thermoelectric effect consists of three effects which are the Seebeck effect, the Peltier effect, and the Thomson effect.

3.1.1. The Seebeck Effect

The Seebeck effect is the conversion of a temperature difference into an electric current, named after the Baltic German Physicist Thomas Johann Seebeck, who discovered it in 1821. He observed that a compass needle would be deflected if connected in a closed loop formed by two different metals joined in two places, with a temperature difference between the joints. Not recognizing that the deflection of the needle was due to an electric current, Seebeck termed this as a magnetic field effect, which was corrected later by a Danish Physicist Hans Christine Ostred who coined the term thermoelectricity (Electrical4u, n.d.).

Figure 3-1 shows two conductors A and B, connected at their ends that are at different temperatures namely hot and cold. A potential difference V is generated.

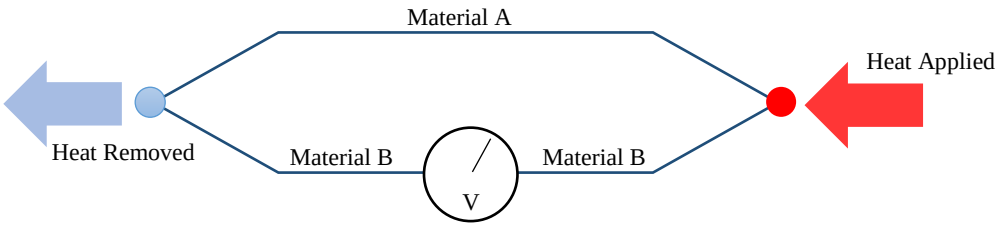

Figure 3-1. The Seebeck Effect

This potential difference V is proportional to the difference in temperatures at the two ends.

$$V = \alpha \Delta T \quad (3.1)$$

Here ΔT is the temperature difference, and α is the Seebeck coefficient and is usually measured in units of µV/K.

3.1.2. Peltier Effect

When a current is passed through a junction between two different metals, heat is either added or subtracted from the junction depending upon the direction of the current (Figure 3-2). This effect is called the Peltier Effect and was discovered by a French Physicist Jean Charles Athanase Peltier in 1834 (FerroTec n.d.). The mathematical form of the Peltier effect is as follows:

$$\dot{Q} = (\Pi_A - \Pi_B)\, I \qquad (3.2)$$

where $\dot{Q}$ is the Peltier heat at the junction per unit time, Π_A and Π_B are the Peltier coefficient of conductors A and B, respectively.

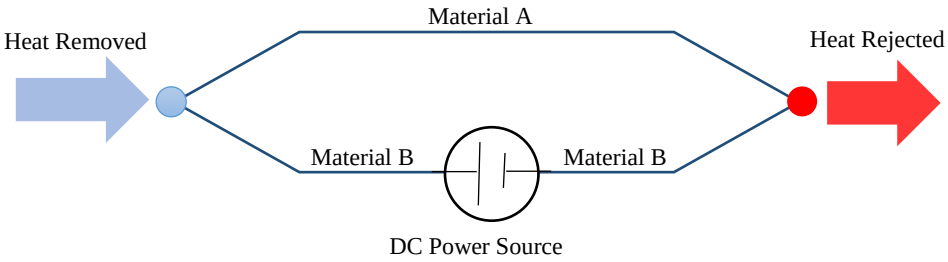

Figure 3-2. The Peltier Effect

3.1.3. Thomson Effect

When a current is made to flow through a conductor with a temperature gradient, heat is absorbed or liberated depending upon the material and the direction of the current. This effect is termed as the Thomson effect and was observed by William Thomson in 1851 (FerroTec n.d.).

Mathematically:

$$\dot{Q} = \tau I \Delta T \qquad (3.3)$$

Here $\dot{Q}$ is the Thomson heat, τ is the Thomson coefficient, I is the current and ΔT is the temperature gradient of the conductor. The Thomson coefficient is unique amongst the three thermoelectric coefficients as it can be measured for individual materials.

Thermoelectric effects were observed in the early 1800s, but their usefulness was realized with the development of the semiconductor industry. Previously, the effect was created by using two different metals, but with the semiconductor p- and n-type materials which are doped to give a different charge density, the materials can be used to form a thermoelement couple or simply a thermocouple.

3.2. Thermocouple

A thermocouple typically consists of one p-type and one n-type semiconductor element, and they are connected to each other with the help of a conductor (e.g., copper) to form a junction. A typical thermocouple is shown in Figure 3-3.

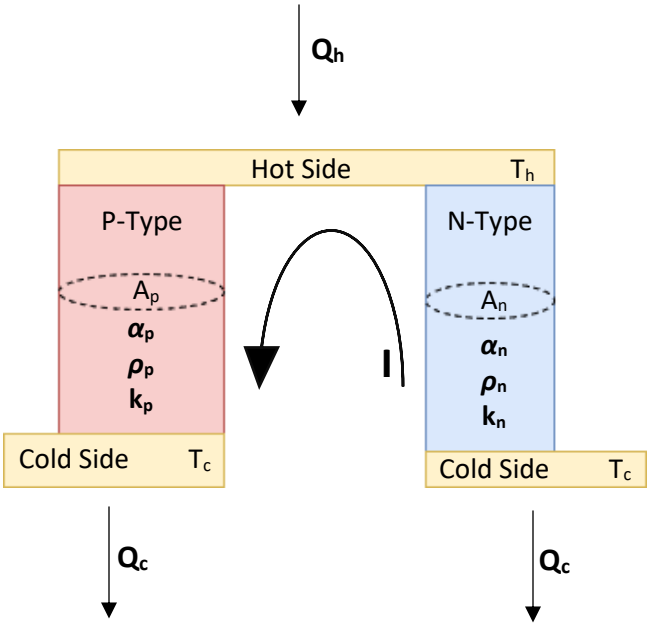

Figure 3-3. A Thermocouple

Where α (μV/K), ρ (Ω m) and k (W/m K) are the Seebeck coefficient, resistivity and thermal conductivity of the respective p-type and n-type semiconductor materials. I (A) is the current flow resulting from the different temperatures at two junctions (The Seebeck Effect).

3.2.1. The Figure of Merit

The performance measurement of thermoelectric devices is done using a figure of merit, Z, where the unit is either $1/^{o}C$ or 1/K for a given material;

$$\mathbf{Z=\alpha^2/\rho k} \qquad \mathbf{(3.4)}$$

Since a thermoelectric device is composed of a single or multiple thermocouples of p-type and n-type semiconductor elements, the convention is to use the following notation.

$$\alpha = \bar{\alpha}_p - \bar{\alpha}_n$$

$$\rho = \bar{\rho}_p + \bar{\rho}_n$$

$$k = \bar{k}_p + \bar{k}_n$$

Here the bar donates an average value over a range of values between the hot and cold junction temperatures. For similar materials the p and n materials are doped in such a way that they give:

$$\alpha_p \cong -\alpha_n$$

$$\rho_p \cong \rho_n$$

$$k_p \cong k_n$$

It must be noted that equation 3.4 is used when p-type and n-type materials are the same; in case of dissimilar materials, the following relationship is used (Lee, 2010).

$$\mathbf{Z= (\alpha_p - \alpha_n)^2 / [(k_p\rho_p)^{1/2} - (k_n\rho_n)^{1/2}]^2} \qquad \mathbf{(3.5)}$$

For the material to have a high value of the figure of merit, it must have a high Seebeck coefficient, a low resistivity (or a high electrical conductivity), and a low thermal conductivity. These are, however, conflicting parameters, and to optimize the performance, there must be a tradeoff. This situation is normally avoided by trying to have a high Seebeck coefficient, as reducing the thermal conductivity of a material is a difficult task (Dresselhaus et al., 2007).

Bismuth telluride (Bi_2Te_3) has a figure of merit equal to 2.5×10^{-3} K^{-1} and has been widely used for thermoelectric cooling along with its alloys, whereas lead telluride (PbTe) with Z equal to 1.3×10^{-3} K^{-1} has been used for thermoelectric generation. Instead of Z, the dimensionless figure of merit ZT is often used as a material characteristic, where T is the average of the temperature of the hot and cold junctions (Lee, 2010).

Zhao et al. (2014) reviewed that the highest ZT value in the literature is about 3 reported by Harman (2005). Thermoelectric-based domestic and commercial heating, ventilation and air conditioning would become practical if ZT value is reached to 2, whereas the current commercially available materials have a ZT value up to 1 (Zhao et al., 2014).

3.3. Thermoelectric Generator

A thermoelectric generator is a solid-state power generation device with no moving parts, where thermal energy converts to electrical energy. The simplest thermoelectric generator consists of a thermocouple of the p-type and n-type semiconductor materials, and the working principle is based on the Seebeck effect. In commercial thermoelectric generators, many thermocouples are electrically connected in series and thermally in parallel between two ceramic plates.

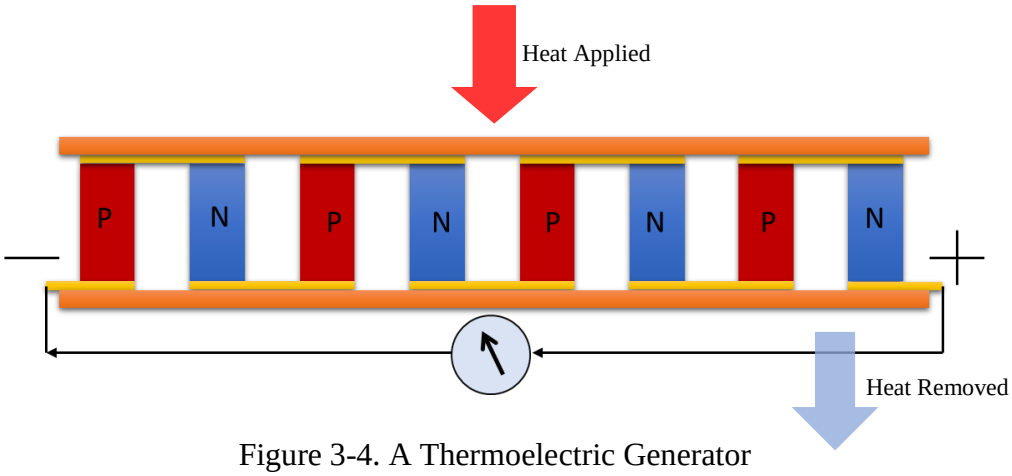

Figure 3-4. A Thermoelectric Generator

At the hot junction, the total heat flow involves the heat associated with the Seebeck effect, the half of the Joule heating, and the thermal conduction (Lee, 2010).

$$Q_h = \alpha T_h I - \frac{1}{2} I^2 R + K (T_h - T_c) \qquad (3.6)$$

Here α is the Seebeck coefficient, R the internal electrical resistance of thermoelements, K the thermal conductance, I the current, and T_h and T_c are the hot and cold junction temperatures, where heat is applied and rejected, respectively, as shown in Figure 3-4.

3.4. Thermoelectric Cooler

The Seebeck effect in a thermocouple shows that a counter effect can be created, which is the Peltier effect as described earlier. The device based on the Peltier effect is called a Peltier cooler or a thermoelectric cooler and is defined as a solid-state heat pumping device with no moving parts, where electrical energy is converted to thermal energy, the simplest of which consists of a thermocouple of the p-type and n-type semiconductor materials.

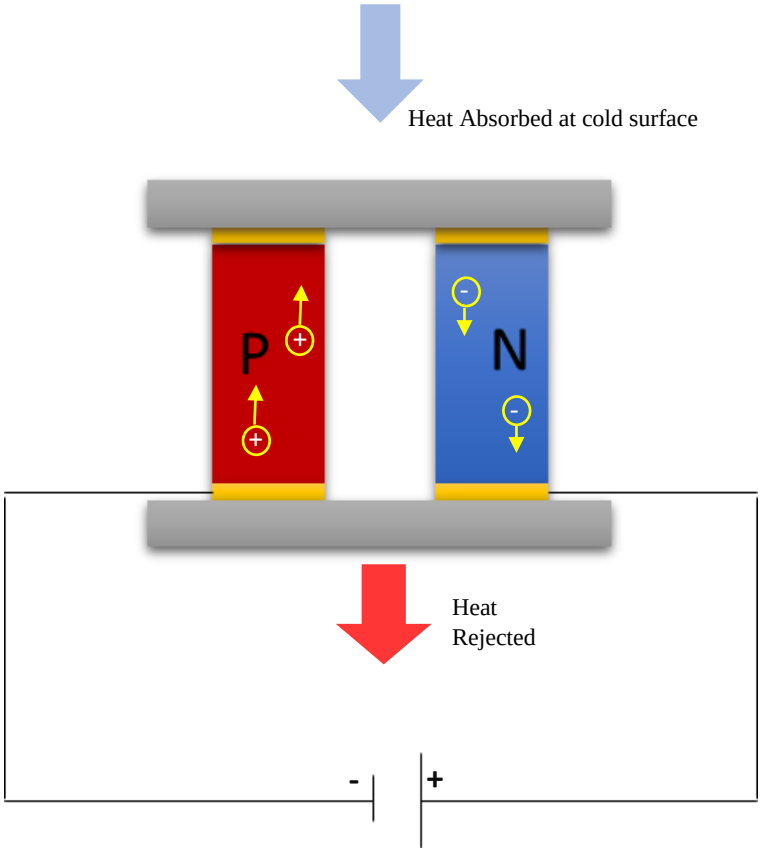

Figure 3-5. A Thermoelectric Cooler

3.4.1. Working Principle

When the current is applied to a thermocouple, the charge carriers in the p-type material, which are at a lower energy state, are forced to move towards the n-type material, a higher energy state.

The required energy is absorbed from the junction resulting in lower temperature at the junction. When these charge carriers are moved from n-type material to p-type material, energy is released, and the temperature of this junction increases. If the direction of the current is reversed, the direction of the heat flow will also be reversed.

3.4.2. Heat Flow in Thermoelectric Cooler

A basic electrical circuit for a thermoelectric cooler (TEC) consisting of one thermocouple is shown in Figure 3-6. The heat absorbed at the cold junction is the resultant of the Peltier heat, the half of joule heating, and the Fourier conduction. The Joule heat and the Fourier conduction are in the opposing direction of the Peltier heat but are inevitable as they are associated with a current flow and a temperature gradient in a conductor which are present in a thermoelectric cooler. The energy balance gives the net heat absorbed at the cold junction (Lee, 2010).

$$Q_c = \alpha T_c I - \frac{1}{2} I^2 R + K (T_h - T_c) \qquad (3.7)$$

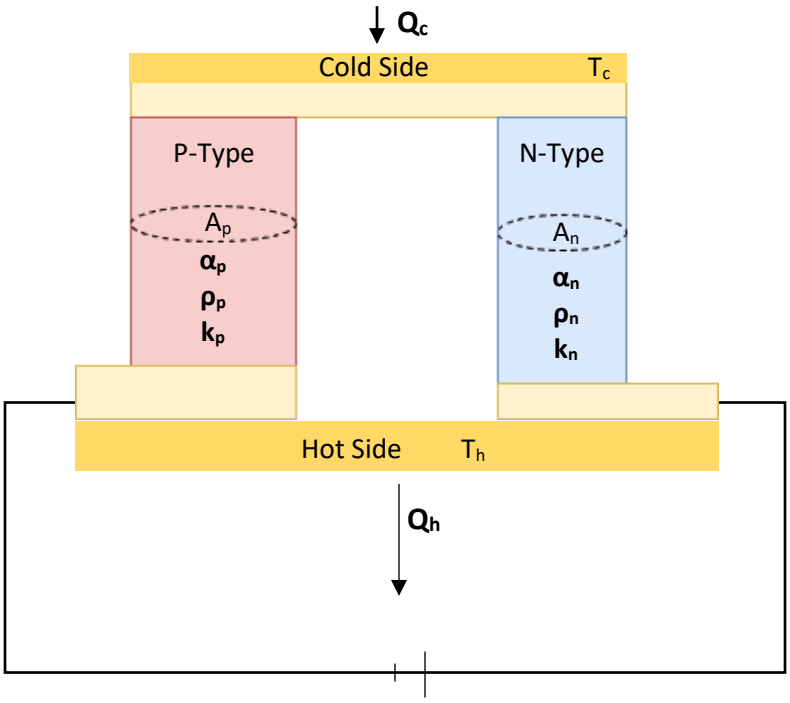

Figure 3-6. Heat Flow in a Thermoelectric Cooler

Here α is the Seebeck coefficient, R the internal electrical resistance of thermoelements, K the thermal conductance, I the current, and T_c and T_h are the hot and cold junction temperatures, where heat is removed and rejected, respectively.

3.4.3. Thermoelectric Module

For the commercial use, many thermocouples are electrically connected in series and thermally in parallel between two ceramic plates. This arrangement is called a thermoelectric module and is shown in Figure 3-7.

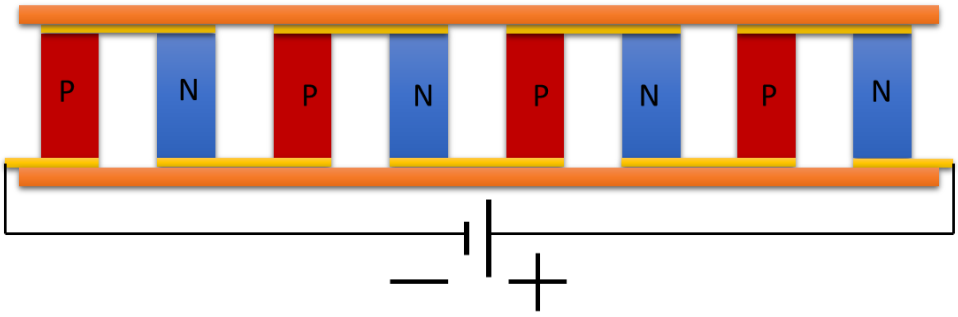

Figure 3-7. A Thermoelectric Module

A thermoelectric module consists of the following components.

(1) A matrix of thermoelectric elements (also called pellets): This matrix is the basic component responsible for the thermoelectric phenomenon in a module. In the commercially available bulk thermoelectric coolers, the p-type and n-type pellets are normally of the same material and the same size. However, for the purpose of performance optimization, different materials and different sizes for a p-type and n-type thermoelement may also be used.

(2) Ceramic plates: These plates are used to insulate the module electrically and to receive or reject the combined heat of thermoelements. These plates also provide the module with mechanical strength. The high thermal conductivity of these plates is essential for module performance. Aluminum oxide (Al_2O_3) is common due to its optimal cost/performance ratio and developed processing technique. Aluminum nitride (AlN) and beryllium oxide (BeO) have much better thermal conductivity, but due to high cost and carcinogenicity of BeO, they are less common.

(3) Electrical conductors: To carry the current from the DC power source and from one thermocouple to the other, electrical conductors in the form of Cu tabs are used.

(4) Solders: Mounting of thermoelements in a module is achieved by soldering. It is the soldering temperature that would determine the operating temperature of the thermoelectric cooler/module.

3.5. Thermoelectric Cooler Performance Parameters

3.5.1. The coefficient of Performance

The coefficient of performance of a thermoelectric cooler is defined by the ratio of the heat pumped at the cold side, Q_c (W), to the input power $\dot{W}$ (Watt). It is similar to thermal efficiency except that it can be greater than 1 (Lee, 2010).

$$\mathbf{COP = Q_c / \dot{W}} \tag{3.8}$$

$$\mathbf{COP = \frac{\alpha T_c I - \frac{1}{2} I^2 R - K\Delta T}{\alpha I (T_h - T_c) + I^2 R}} \tag{3.9}$$

3.5.2. Optimum Current for the maximum cooling rate

The net heat absorbed at the cold junction is given as (Lee, 2010):

$$\mathbf{Q_c = \alpha T_c I - \frac{1}{2} I^2 R + K (T_h - T_c)} \tag{3.10}$$

To get the current optimized maximum cooling rate, differentiate Equation (3.10) with respect to I and set it equal to zero. The optimum current after solving for I is:

$$\mathbf{I_o = \frac{\alpha T_c}{R}} \tag{3.11}$$

3.5.3. Maximum Performance Parameters

Maximum Current (I_{max}): It is the maximum value of the current or the voltage to achieve the maximum temperature difference. Equation 3.12 is the maximum current for a given material and geometry.

$$\mathbf{I_{max} = \frac{\alpha T_c}{R}} \tag{3.12}$$

Maximum temperature difference (ΔT_{max}): It is the maximum temperature difference that can be achieved across the module between the hot side and the cold side. $\mathbf{\Delta T = \Delta T_{max}}$ when $\mathbf{Q_c = 0}$, and $\mathbf{I = I_{max}}$

$$\mathbf{\Delta T_{max} = \alpha^2 T_c^2 / 2KR} \tag{3.13}$$

Maximum Cooling Rate ($Q_{c\ max}$): It is the maximum heat that can be pumped from the cold side for a given thermoelectric cooler. $\mathbf{Q_c = Q_{c\ max}}$ at $\mathbf{\Delta T=0}$.

$$\mathbf{Q_{c\ max} = K\Delta T_{max}} \qquad \mathbf{(3.14)}$$

3.5.4. Generalized Performance Charts for a thermoelectric cooler

The performance of the thermoelectric cooler is conveniently predicted in the forms of charts rather than constituting the material properties and geometry. To express the n dimensionless form of parameters, they are divided by their maximum value and then plotted to observe the relationship to each other as can be seen from the following graph (Lee, 2010).

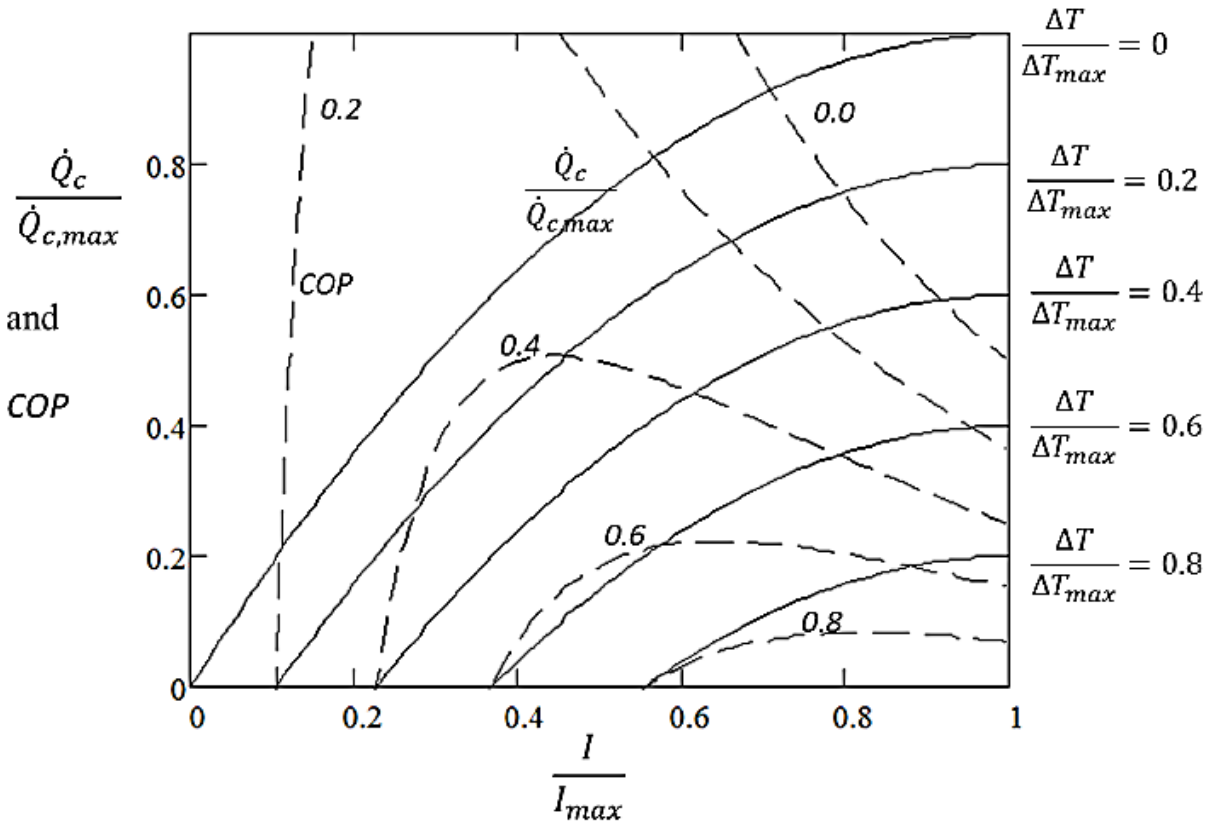

Figure 3-8. Generalized Chart for a single stage thermoelectric cooler (Lee, 2010). Reproduced with permission

3.6. Multistage Thermoelectric Coolers

Single stage thermoelectric coolers can achieve up to a certain value of temperature difference. However, in many applications, an even greater temperature difference is required. Multistage thermoelectric coolers are employed to achieve this requirement, where each lower stage acts as a heat sink for the upper stage. This structure is also called cascading and may result in a pyramid shape or for two-stage coolers, where the two stages are with the same length and width but different height.

3.7. Heatsink for thermoelectric coolers

A thermoelectric cooler is a solid-state heat pumping device which means it takes heat from the cold side and rejects it towards the hot side along with the Joule heat arising due to the current passing through TEC. As a result, the temperature of the hot side increases. For this cooler to continue its operation, the hot side temperature needs to be maintained, and heat must be rejected to ambient through a heatsink. The heatsink is an important part of a thermoelectric cooling system and plays a great role in the performance of the thermoelectric cooling system.

In each of the thermoelectric cooling applications, a unique heatsink and cooling technology would be required. Natural convection is effective for low current carrying small modules. But as the input current and heat load increases, forced convection, phase change cooling and liquid cooling may become necessary.

Chapter 4

Thermoelectric Cooling for Dental Pulp Testing

Thermoelectric coolers are the solid-state heat pumping devices and offer numerous benefits over their counterparts. They are maintenance and noise free as they do not have any moving parts. Their small size and weight in comparison to mechanical systems, and ability to both heat, and cool below 0℃ make them unique in many applications. They have precision at the order of +/- 0.1°C and are highly reliable. They can operate in any orientation and are environment-friendly (Ferrotec Nord Corporation, n.d.).

4.1. General Applications of Thermoelectric Cooling

Thermoelectric cooling finds extensive applications in thermal management, heating, ventilating and air conditioning, and medical devices where one or more advantages of thermoelectric cooling are utilized. For the current scope of work, this chapter will review their use in Medical Devices generally and for Cold Pulp Testing in detail.

4.1.1. Thermoelectric Cooling in Medical Devices

Thermoelectric Refrigerators: Medical devices utilize one or more of the advantages of thermoelectric cooling. Due to their high reliability and precise temperature control TE cooling is used in vaccine storage and transport. Small size and scalability to micro level make thermoelectric cooling a potential solution for miniature refrigeration systems which are not possible through conventional mechanical systems (Chen, 2012).

Therapeutic Applications: Thermoelectric cooling can be directly used to provide the patient with cooling as required due to their precise temperature control. These applications also involve the treatments of tissue injuries (Chen, 2012). Natalia et al. reported the effectiveness of thermoelectric coolers in the treatment of soft tissue injuries by alternating between high and low temperatures (Natalia et al., 2015).

Polymerized Chain Reaction (PCR): One of the most important and oldest applications of thermoelectric cooling is PCR. It was developed in 1983 by Biochemist Kary Mullis who was later

awarded a Nobel prize in Chemistry. Rapid cooling and heating is provided through thermoelectric phenomena for DNA amplification (Chen, 2012).

Biological Micro-electromechanical systems (BioMEMS): Recent developments in the MEMS industry have paved the way for portability and on-site care in biomedical devices. Though the current utilization of micro thermoelectric coolers in the lab on a chip is limited to the rapid thermal cycling for the polymerized chain reaction (PCR) only, the future trends in MEMS predict an increase in their usage (Chen, 2012).

4.2. Thermoelectric Cooling for Cold Testing of Dental Pulp

Chapter two discussed dental pulp testing, its importance and how cold testing of the dental pulp is the most accurate of all the pulp testing techniques but current methods and materials for cold testing are a potential hazard to patient safety and clinically difficult to adopt. Thermoelectric coolers provide precise control, scalability, and portability for on-site applications. This gives an opportunity to utilize thermoelectric cooling for cold testing of the dental pulp, hence eliminating the potential safety hazards associated with the conventional methods and acquiring more confidence over diagnostic results.

4.2.1. Previous Research

Previous work concerning dental pulp testing by a group of undergraduate students from the Mechanical Engineering department at the University of Saskatchewan is worth mentioning. The work studied the possibility of using thermoelectric cooling to bring the temperature of air to 7℃ in a tank, this air was then cooled down to -35℃ by a vortex tube, and the air was to finally be blown on to the tooth for the pulp sensibility testing purpose (Brown et al., 2016). However, this approach could be harmful to the patient as the cooled air might damage the skin tissues inside the mouth or oral cavity; as well, there was a loud sound created in the blowing process.

Thermoelectric Pulp Testing Devices: Patented on May 19, 1964, for Inventor William Eidus, a Thermoelectric Medical Instrument was presented. It was a hand-held, stand-alone device and a water reservoir was used for cooling down the thermoelectric element.

Patented October 13, 1976, for Inventor Jordan M. Scher under the title “Diagnostic Instrument used in Testing Patient Response to Heat, Cold and Electrical Stimuli” was based on a

thermoelectric element as well. Again, it was handheld and could produce heat, cold and electrical shock; however, it required different modules to do so, and the design did not discuss any heat dissipation from the thermoelectric element.

Patented on January 1, 1974, for Inventor Ronald W. Brown under the title “Dental Pulp Tester” was a Thermoelectric Dental pulp tester which could provide heat, cold, electric shock, and mechanical impact. This device was handheld too and used an n-Butane Tank for Heat dissipation.

Patented on December 29, 1981, for Inventor Emery Major under the title “Thermoelectric Diagnostic Instrument” was handheld to provide heating and cooling and had a heatsink for heat dissipation under forced convection.

On September 21, 1982, the inventor Laurance B. Davis issued a patent for a dental pulp tester. This tester used a thermoelectric cooling module, and a liquid cooled heat sink. The limitation of this tester is that it was not stand alone, as it was a liquid cooling device and water was going inside and coming outside through the water channels in the device.

Patented March 6, 2001, for inventor Robert Gregg Ross under the title “Continuous use Orthodontic Cooling Appliance” provided more time of operation but it was not stand-alone, as it used water channels going in and out of the device for cooling down the thermoelectric element.

In summary, all the devices mentioned above were essentially based on thermoelectric cooling for the dental pulp testing, but they differ in the heat dissipation method used for sinking the heat from the hot side of the thermoelectric cooling element.

4.2.2. Challenges in achieving a new portable thermoelectric pulp testing device

In the introduction to thermoelectric cooling (Section 3.7), a thermoelectric cooler must be used in conjunction with a suitable heatsink, hence forming a thermoelectric cooling system together. The heat load at the hot side of the thermoelectric cooling system may range up to 100W depending upon the consumption of power by TEC. Without using a heatsink, it is not possible to use the thermoelectric cooler up to its full potential, i.e., a stand-alone and portable pulp testing probe. The heatsink for a thermoelectric cooler may be based on one of the following heat dissipation principles:

1. Air Cooling (Natural Convection, Forced Convection),

2. Liquid Cooling, and
3. Phase Change Cooling (Heat Pipes, Vapor Chamber).

The subsequent chapter will review the literature to establish an understanding and comparison of these cooling methods for their use in the thermoelectric dental pulp testing device.

Chapter 5

Heatsink Considerations for Thermoelectric Cooling Systems

Heatsink size is a key factor in miniaturizing the whole device. The contact area is an important factor in heat dissipation. A lot of solutions have been proposed to address the issue of the contact area in the literature, starting from the cold plate through fins to heat pipes and heat spreaders, and to their combination for achieving a required heat dissipation. However, when it comes to a device which rejects a lot of heat in a small area, heat sinking becomes a challenge due to a small contact area for heat transfer. The concepts such as vapor chamber and micro heat pipes have been recently proposed, and they are an effective way to dissipate heat even in a smaller area. Micro channel heat exchangers are an example of liquid cooled microdevices (Lee, 2010).

All of these heat dissipation methods are based on a basic principle – i.e., increasing the contact area. Till date, the most efficient methods are the liquid cooling, where a refrigerant or coolant comes in contact with the surface to be cooled. The liquid must be pumped into channels, and thus the presence of the pump contributes to the large size of such devices. Heat pipes, which are put intermediate to the air and extensive cold liquid are an effective way of heat dissipation, as they use a fluid (mainly water) as a coolant and do not require a pump for the circulation. The circulation in the heat pipe technique is achieved by the phase change, as the water evaporates and condenses just under the influence of the force of gravity and capillary force. The internal wick structure of the heat pipe provides this required capillary action. The conventional air cooling methods (both free and forced convection) cannot be relied upon for their high heat fluxes and are thus being replaced by micro channel heat exchangers or heat pipes. However, they may still be used in combination with the micro channel heat exchanger or heat pipe technique to dissipate the heat into the ambient more reliably and efficiently.

A cooling system or device that is based on TEC and can achieve a cryogenic temperature of the order of -60℃ for medical purposes still needs to be investigated. This chapter will provide a brief introduction to thermal management techniques that can be used in conjunction with thermoelectric coolers and will discuss phase change cooling methods in detail concerning this study.

5.1. Air Cooling

Natural Convection: This is perhaps the simplest technique and can dissipate up to 5 Watts effectively in circuit boards (Anandan et al., 2008). Natural convection is still used in applications where sufficient ambient air flow is available due to its low cost and established manufacturing controls.

Forced Convection: When available air flow is not sufficient, forced convection is used for cooling using a fan or a blower. Two parameters are used to characterize a fan for an application: (A) Static Pressure Head and (B) Volume flow rate.

These techniques may be directly used for the heat dissipation of a component or may be used in combination with a heatsink. Anandan et al. (2008) reviewed heatsink enhanced natural and forced convection and reported that the geometry of the heatsink and type of airflow used has a significant impact on the heat transfer.

5.2. Liquid Cooling

Liquids have higher heat transfer coefficients than gases, which makes liquids more suitable for applications where air cooling, both forced and free convection, is unable to achieve the required heat dissipation. But liquid cooling comes at the cost of more weight and corrosion due to the leaking of the liquid from the channels, and that is why they are limited to high power density applications only, where other thermal management techniques are no more effective. Liquid cooling is achieved by using one of the following approaches:

A) Immersion Cooling,
B) Boiling Heat Transfer,
C) Jet Impingement, and
D) Spray Cooling.

5.3. Phase Change Cooling

Phase change cooling in electronics is achieved through heat pipes or heat spreader/vapor chamber. They utilize the phase change of the working fluid, where the fluid takes its latent heat of vaporization from the component being cooled to evaporate and then to release this heat at the condenser section to become liquid again. From here the liquid returns to the evaporator section

either by gravity or by the capillary action of the wick structure in the device. The simplest one of the phase change cooling systems is based on water and copper and has two concepts: (A) heat pipe and (B) vapor chamber.

5.3.1. Heat Pipes

The heat pipe is a device that has no moving parts and is composed of three sections: evaporator section, condensation section, and an adiabatic section between the evaporator section and condensation section. Heat pipes are as capable of transporting the heat flux as the latent heat of vaporization of the working fluid (Chen et al., 2015).

Heat pipes can be bent in any orientation and can be used to take heat away from the hot component to a remote condenser. However, heat pipes transport heat only along their length and hence offer some thermal resistance in the lateral direction. Figure 5-1 presents a heat pipe embedded in a heatsink that shows the x-direction heat conduction is limited.

Figure 5-1. Heat pipes and thermal spreading resistance

5.3.2. Vapor Chambers

While heat pipes spread heat along their length, a vapor chamber is based on the same working principle as the concept of heat pipes and spreads heat in all the directions and therefore the vapor chamber is commonly referred to as the heat spreader. In addition to spreading heat in all directions, vapor chambers offer more condensation area, as shown in Figure 5-2.

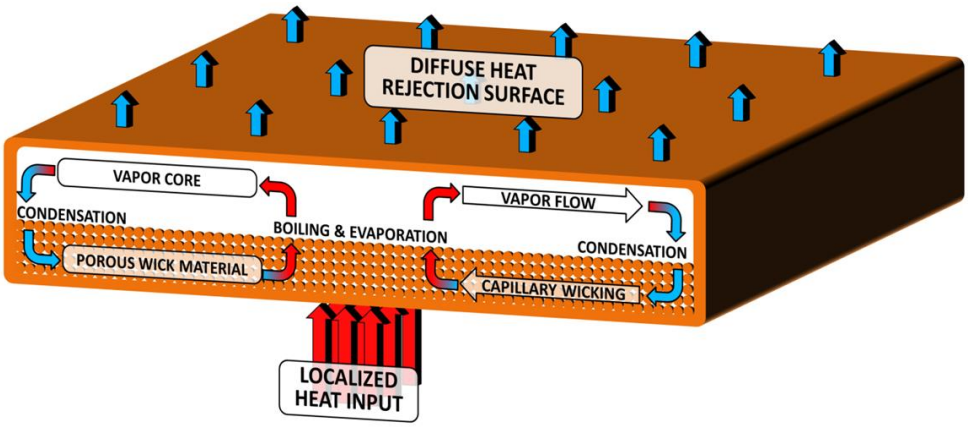

Figure 5-2. Working of a vapor chamber (Weibel et al., 2013). Reproduced from open access journal

5.4. Conclusion

The phase change cooling methods are passive cooling methods, i.e., they do not require any input power or moving parts, and hence they provide lightweight and compactness in the devices. In terms of cost, they are cheaper than liquid cooled heatsinks. Due to these features, only phase change cooling methods (heat pipes and vapor chamber in particular) were studied with the thermoelectric cooler in this study to develop a thermoelectric dental pulp testing device. However, if the heat load is too high to control by any of the phase change cooling methods, extensive liquid cooling may become necessary.

Chapter 6

Feasibility Study of Phase Change Cooling Methods

In this chapter, the experiments are described to study the feasibility of using the thermoelectric cooler along with the phase change cooling method for the dental pulp testing device. It is noted that the requirement for the device was described in Chapter 1 – to achieve -60^{o}C in particular. The general strategy for the experimental study was to take the off-the-shelf systems whenever possible considering the cost-effectiveness and reliability of the device as well as pilot nature of the study.

6.1. Materials and Methods

6.1.1. Thermoelectric Coolers

Thermoelectric coolers are available commercially from a number of suppliers. They are categorized either as bulk technology modules that utilize pellets of thermoelectric elements ranging from 1 mm thermoelement length to a few millimeters or thin film technology for miniaturized thermoelectric coolers.

Thermoelectric coolers for the dental pulp testing device would be customized regarding their size and parameters for this application specifically. However, some commercially available thermoelectric coolers can provide the idea of the effectiveness of thermoelectric coolers for the pulp testing device and challenges that may arise in the later stages of the design.

Product catalogs of leading manufacturers of thermoelectric coolers around the world were searched, and some thermoelectric coolers were shortlisted for testing. The following selection criteria were derived from the overall requirement of the pulp testing device (see the previous discussion in Section 1.3) and were used for the selection of proper thermoelectric coolers:

-Size (maximum 50×50 mm^2 in area),
-Cost (less than CAD 50 for a single module),
-Temperature difference (dT_{max}) should be at least 70^{o}C,
-Availability (available as a single unit), and
-Lead time (maximum 30 days).

The thermoelectric coolers along with their important properties concerning testing are listed below and are named as 1 and 2 for this study.

Thermoelectric Module 1

Manufacturer Name: TE Technology Inc.

Name in Manufacturer's Catalogue: VT-127-1.4-1.5-72

The properties of this thermoelectric module are presented in Table 6-1 along with the schematic diagram in Figure 6-1.

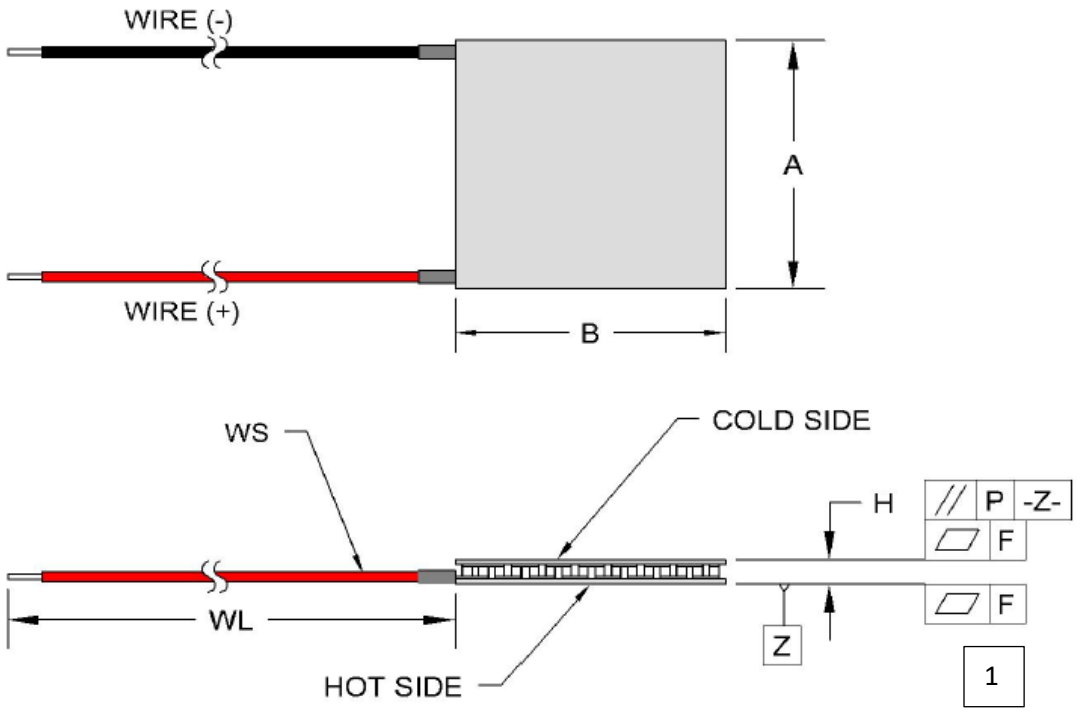

Figure 6-1. Thermoelectric Module 1 (Used with permission from TE Technology)

Table 6-1. Properties of thermoelectric module 1 (From TEC Datasheet)

Parameter	At T_h = 27°C	At T_h = 50°C
V_{max} (V)	16.3	18.1
I_{max} (A)	6.1	6.1
Q_{max} (W)	62	68
DT_{max} (°C)	72	81

Width A (mm)	40	40
Width B (mm)	40	40
Height H (mm)	3.9	3.9
Flatness F (mm)	.02	.02
Parallelism P (mm)	.03	.03
Wire size WS (mm^2)	.34	.34
Wire length WL (mm)	124	124

Thermoelectric Module 2

Manufacturer Name: TE Technology Inc.

Name in Manufacturer's Catalogue: TE-2-(31-12)-1.0

The properties of this thermoelectric module are presented in Table 6-2 along with the schematic diagram in Figure 6-2.

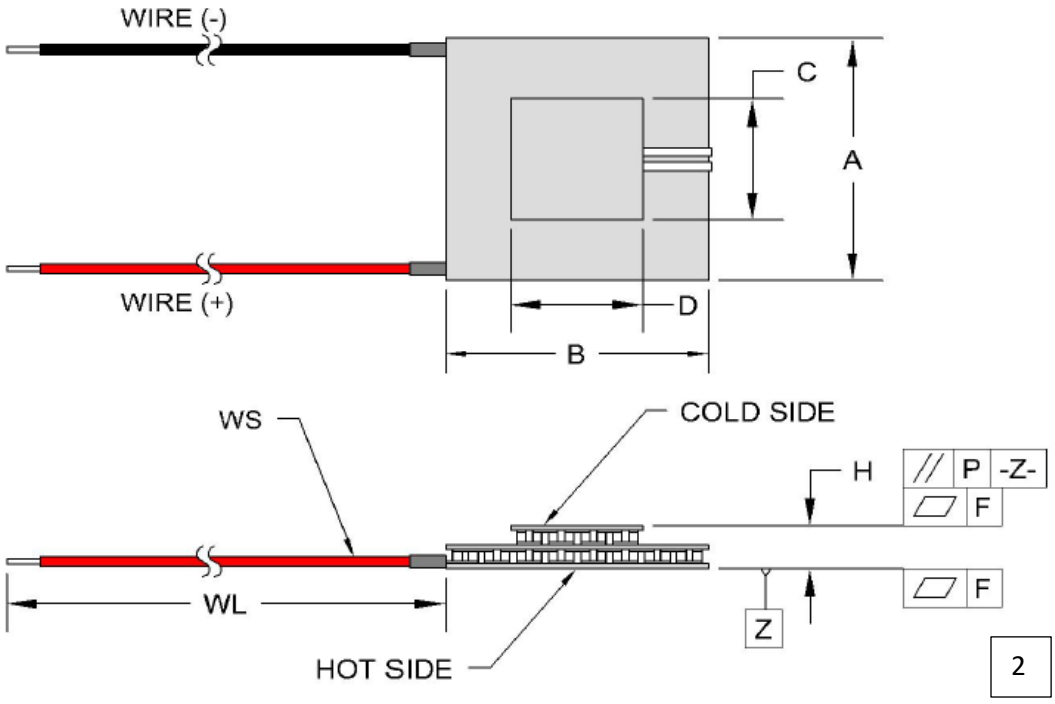

Figure 6-2. Thermoelectric Module 2 (Used with permission from TE Technology)

Table 6-2. Properties of thermoelectric module 2 (From TEC Datasheet)

Parameter	At T_h = 27 ^oC	At T_h = 50 ^oC
V_{max} (V)	3.7	4.1
I_{max} (A)	1.4	1.4
Q_{max} (W)	1.6	1.8
DT_{max} (^oC)	91	103
Width A (mm)	8	8
Width B (mm)	10	10
Width C (mm)	4	4
Width D (mm)	6	6
Height H (mm)	5.35	5.35
Flatness F (mm)	.1	.1
Parallelism P (mm)	.15	.15
Wire size WS (mm^2)	.2	.2
Wire length WL (mm)	120	120

6.1.2. Phase Change Heatsinks

As discussed in Chapter 3, the heatsink is an essential part of a thermoelectric cooling system, and a thermoelectric cooler should be used with a heatsink. A wide range of heatsinks is available commercially, but the heat load estimated for the thermoelectric coolers from the information of input current and voltage to the respective TEC from its data sheet (see the next section for details) shows that the conventional cooling techniques of both natural and forced convection would be unable to dissipate these heat loads while maintaining the dimensional constraints of the dental pulp testing device. The phase change cooling method was next employed to understand their capabilities to dissipate these high heat loads.

The following phase change heatsink consisting of 3 heat pipes was tested with the thermoelectric modules. It is noted that the following criteria were used for the selection of the proper heatsink:

- The integrated heat pipe (must have at least one integrated heat pipe),
- Cost (less than CAD 80 for a single unit),

- Airflow (must be integrated with a fan),
- Availability (available as a single unit), and
- Lead time (maximum 30 days).

The schematic of the heatsink along with the manufacturer specifications is discussed below.

Heatsink 1 (there is the other heatsink, Heatsink 2, to be discussed later):

Manufacturer: ZALMAN

Name in Manufacturer's Catalogue: CNPS7X LED+

Table 6-3. Properties of heatsink 1 (From Heatsink Datasheet)

No. of Heat Pipes	3 direct touch heat pipes
Fin Material	Aluminum fin stack
Fan Speed	1350-2100 RPM
Dimensions	104(L) × 85(W) × 134(H)mm
Weight	360 g

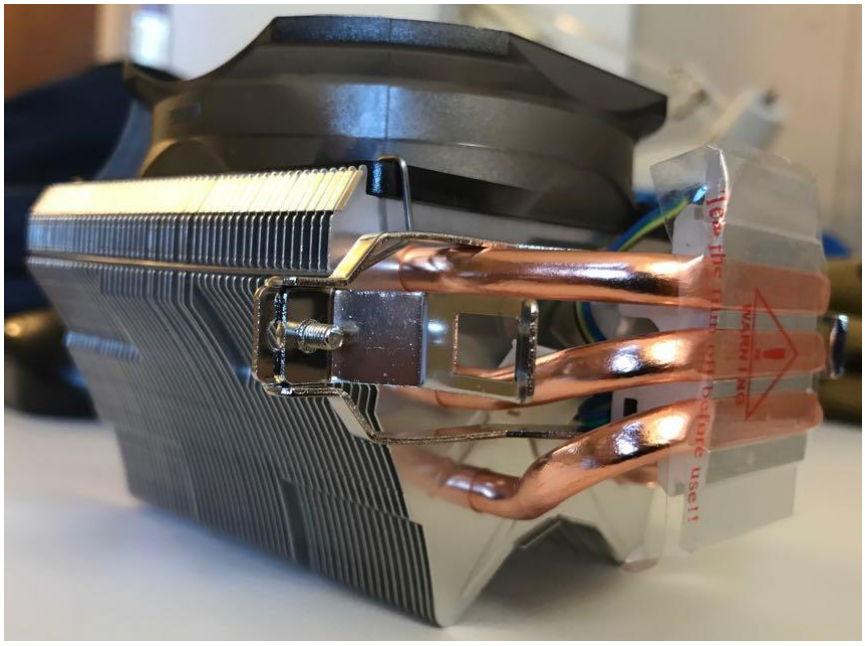

Figure 6-3. Heatsink 1

6.1.3. Experimental Setup

The test-bed was composed of a 0-20V DC bipolar power supply (KEPCO, Inc.), two type 'K' thermocouples (OMEGA ENGINEERING, Inc.) and an IR thermal imaging camera (E series, FLIR Systems, Inc.). It should be noted that the minimum temperature that the IR thermal imager can measure is -40℃ and is solely used to get the temperature profile rather than the temperature measurement of the system at a point, observing how one area is warmer than the other areas.

The variable power supply was used because different components require different voltages for their operation and type 'K' thermocouples were used because the measured temperature may be in the cryogenic range. The thermocouple (W=1mm, L=3mm) used has a temperature measurement range of -200℃ to 1372℃ with the precision of 0.1℃ and accuracy of $\pm$ (.05% of reading + 0.3℃). The uncertainty in the temperature measurement was calculated and put in Appendix A.

For the testing of a specific TEC, the TEC was placed on the heatsink with a thermal interface material (TIM) between them. The purpose of TIM here was to fill any asperities between the mating surfaces of the TEC and the heatsink as well as to fill the air pockets on the interface. The thickness of the TIM layer and its thermal conductivity are important factors. The thermal resistance at the interface and the thickness of TIM had a linear relationship and using a thicker film means increasing the thermal resistance. Careful consideration should be given to the selection of the TIM. The thermal interface materials usually had a thermal conductivity from 0.1 to 7 W/mK (Blazez, 2016).

In this experimental setup, the TIM was ZM-STG2M (ZALMAN Tech Co., Ltd.) with a thermal conductivity of 4.1 W/mK and based on the experience the film thickness was no more than 1 mm.

Two type 'K' thermocouples were used to measure the temperature at the cold side and the hot side of TEC, respectively. The IR thermal imaging camera was used to take a picture of the system to visualize the temperature distribution. The whole schematic setup of the test-bed is shown in Figure 6-4, and the actual set-up of the apparatus is shown in Figure 6-5.

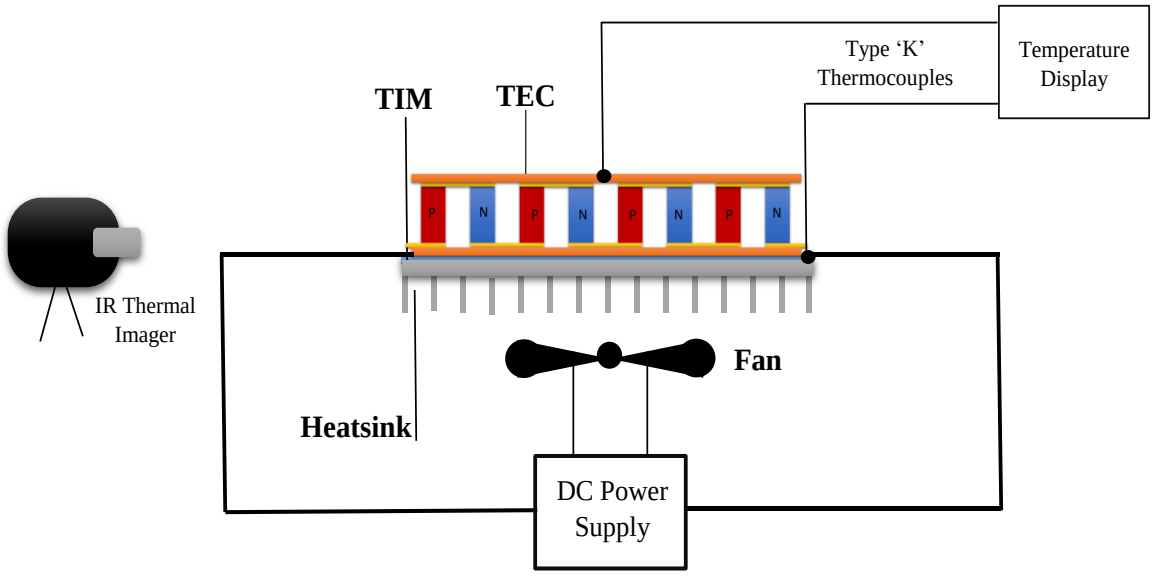

Figure 6-4. Experimental setup for testing of TEC

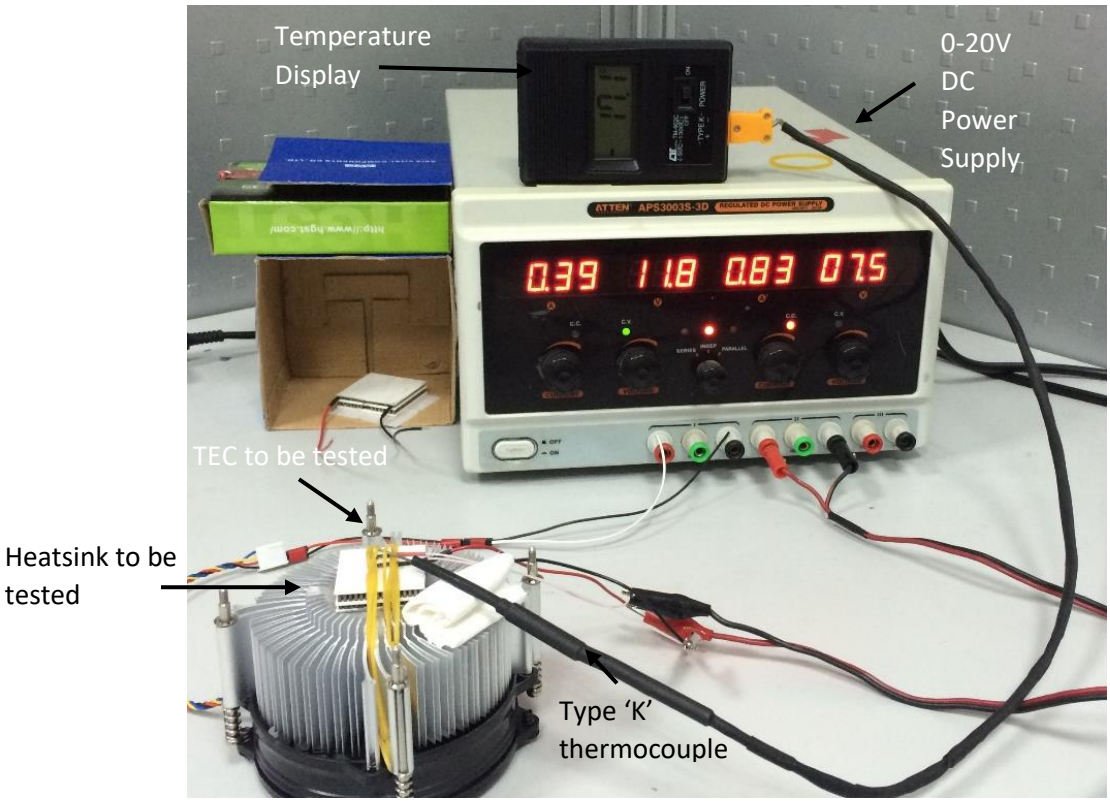

Figure 6-5. The apparatus for testing of TEC

With two TECs and one heat pipe based heatsink, all the possible combinations of the heatsink and TECs were tested; i.e., TEC 1 with the heatsink 1, TEC 2 with the heatsink 1 and both TEC 1 and TEC2 (TEC 2 on top of TEC 1) with the heatsink 1.

In the first experiment, *TEC 1* and *Heatsink 1* were used as per the experimental setup, and temperature measurements were performed. The heat load to be dissipated by the heatsink was denoted as Q_h and calculated by the electrical power consumed by the module. The maximum values of current I and voltage V were not applied (but 75% of the I_{max} and V_{max}) for the steady-state operation to avoid the overheating of the module in the steady-state operation, as recommended by the supplier. During the testing, the voltage was set to the desired value, and the corresponding current was observed. The heat load for a thermoelectric cooling system is given by (Lee, 2010).

$$\mathbf{Q_h = Qc + W_{in}} \qquad \mathbf{(6.1)}$$

Where Q_h is the heat load and Q_c is the heat removed at the cold side of TEC. W_{in} is the electrical power input to the module. At Q_c= 0 Watts, $Q_h = W_{in}$, For Module 1, $W_{in} = V \times I = 12 \times 4 = 48$ Watts. It is noted that the V and I were measured as described before.

It should be noted that there is a systematic uncertainty in both the voltage and current readings, as calculated in Appendix A. However, they may be ignored as the purpose of input power measurement in this study was just to highlight a relative difference in the heat load.

In the second experiment, *TEC 2* and *Heatsink 1* were used as per the experimental setup, and temperature measurements were performed. The heat load to be dissipated by the heatsink was denoted as Q_h and calculated by the electrical power consumed by the module. The maximum values of current I and voltage V were not applied (but 75% of the I_{max} and V_{max}) for the steady-state operation as explained before.

From Equation 6.1, we obtain: at Q_c= 0 Watts, $Q_h = W_{in}$, where W_{in} is the electrical power input to the module. For Module 2, $W_{in} = V \times I = 3 \times 1.27 = 3.81$ Watts. It is noted that the voltage V and current I were measured as described before.

In the third experiment, *TEC 1 and TEC 2* (together) were used with *Heatsink 1* as per the experimental setup, and temperature measurements were performed. The heat load to be dissipated

by the heatsink was denoted as Q_h and calculated by the electrical power consumed by both the TECs. It is noted that both TECs were tested in this experiment, so the total power is: $W_{in\ (total)}$ = 3.81 + 48 = 51.81 Watts.

6.2. Results and Discussion

When the circuit was closed, the temperature at the cold side of TEC started to decrease while the temperature at the hot side of TEC started to increase. For each experiment, five measurements were taken at the steady-state. The steady-state was captured by observation – in particular when there was no fluctuation in temperature at the display and stayed there for at least five minutes. It is noted that the importance of taking a steady-state reading is that it is much closer to the real situation of the dental pulp testing.

Table 6-4 shows the results of all three tests. The given temperatures are the average values of the measurements; however, there is some uncertainty in the measurement primarily due to contact of the thermocouple with the surface at which the temperature was measured. The detailed uncertainty analysis, including the error arising in the interface, is presented in Appendix A.

Table 6-4. Experimental Results

No.	**Module(s) and heatsink configuration**	**Heat Load Q_h (Watts)**	**Cold Side Temperature T_c (^oC)**	**Hot Side Temperature T_h (^oC)**
Experiment 1	TEC 1 with Heatsink 1	48.00	-28.3	51.0
Experiment 2	TEC 2 with Heatsink 1	3.81	-32.5	23.5
Experiment 3	TEC 2 on top of TEC 1 with Heatsink 1	51.81	-56.5	53.0

From this table, it can be seen that the test one can achieve a high-temperature gradient (with one stage TEC only), but the temperature at the hot side T_h of TEC goes above 50℃. It is noted that TEC module 1 is with high power. Figure 6-6 shows the IR thermal image of test one – particularly at a spot near the hot side of TEC.

From Table 6-4, it can be seen that the test two (TEC 2) consumes a very low power but achieves a lower temperature at the cold side than TEC 1. TEC 2 is a two-stage cascaded TEC, and this suggests that the cascaded TEC is promising. The IR thermal image of test two is shown in Figure 6-7.

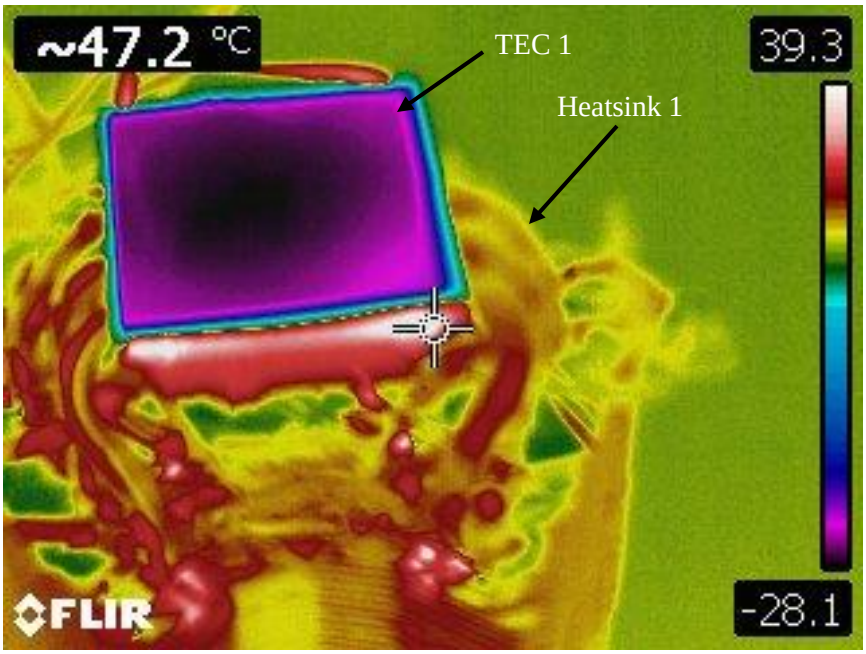

Figure 6-6. IR thermal image of test one

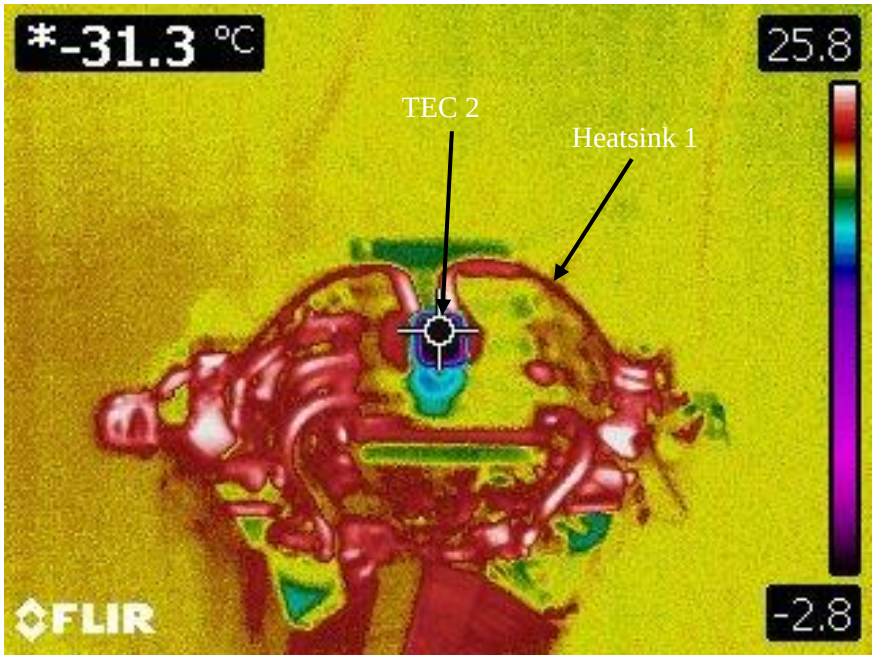

Figure 6-7. IR thermal image of test two

In test three, where both TEC 1 and TEC 2 were used with the heatsink 1, the temperature T_c at the cold side reaches -56.5℃, which is very close to the target value of -60 ℃ for the pulp testing; however, the temperature at the hot side is very high (i.e., 53.0℃) as opposed to the allowed temperature of 40℃ in the pulp testing (see Appendix D for the details of this remark). The IR thermal image of test three is shown in Figure 6-8(a) and 6-8(b).

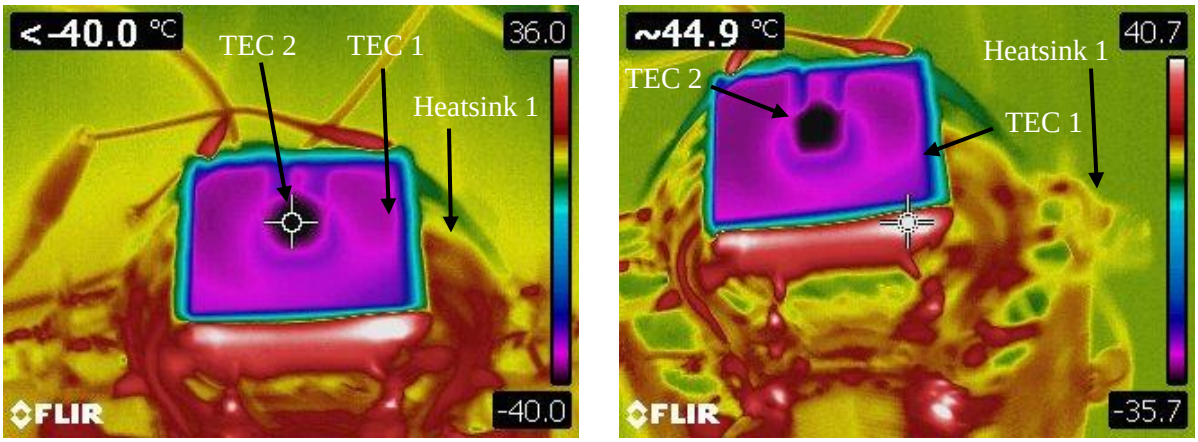

(a) (b)

Figure 6-8. IR thermal image of test three

6.3. Conclusion

The following conclusion can be drawn from the experiment. The cold pulp testing device with the temperature of -60℃ at its probe is feasible to design and fabricate, but such a device needs a customized TEC along with a customized heatsink (as the temperature at the hot side can be as high as 50℃, which is unacceptable from the point of view of the patient's safety). The next chapter is devoted to the discussion of the design of a customized TEC along with a customized heatsink.

Chapter 7

Design of Thermoelectric Cooling Systems

In this chapter, the design of a customized thermoelectric cooler and a customized heatsink is described to achieve the primary requirement of (1) cold temperature (-60^{o}C) and (2) stand-alone portable pulp testing probe. The approach is a simulation-based one. In Section 7.1, the validation of the simulation tool, i.e. Comsol Multiphysics is first presented by simulating an off-the-shelf TEC and comparing its simulation results to the already known experimental data. The result of the comparison fortunately shows that the simulation tool is accurate enough. In Section 7.2, the design of the thermoelectric cooler with the help of the Comsol simulation system is presented, followed by the design of a cascaded cooler in Section 7.3. In Section 7.4, the model verification of the cascaded cooler is presented. In Section 7.5, the design of the heatsink is presented, followed by the experimental validation using an off-the-shelf vapor chamber and TEC in Section 7.6. In the final section (Section 7.7), a conclusion is drawn.

7.1. Simulation Model Verification

Before a simulation model can be utilized, verification of the accuracy of the simulation model must be conducted. In this study, a simulation tool called Comsol was employed. The fundamental theory behind Comsol is the finite element method for multi-physics, where after physical interfaces are defined, a number of elements are created to discretize the governing equations on the interface. To build a Comsol model, one needs to define the geometry, the interface of multi-physics, and the mesh. In this study, the thermal dynamics and electronics are two different domains of physics. The governing equations in this case are given below (Comsol version 5.2a, 2016).

The equation for energy conservation for the heat transfer rate is:

$$\rho C_p \mathbf{u}. \nabla T + \nabla . \mathbf{q} = Q + Q_{ted} \quad (7.1)$$

$$\mathbf{q} = -k\nabla T \quad (7.2)$$

For the thermal insulation:

$$-\mathbf{n} . \mathbf{q} = 0 \quad (7.3)$$

The electric current conservation equations are utilized to calculate the electric field and the current density as follows:

$$\nabla \cdot j = Q_{j.v} \quad (7.4)$$

$$j = \sigma E + j_e \quad (7.5)$$

$$E = -\nabla V \quad (7.6)$$

For the electrical insulation:

$$n.j = 0 \quad (7.7)$$

For the terminal current we have:

$$\int j.ndS = I_0 \quad (7.8)$$

The above equations are coupled to give thermoelectric cooling as follows:

$$q = Pj \quad (7.9)$$

$$P = ST \quad (7.10)$$

$$j_e = -\sigma S \Delta T \quad (7.11)$$

In the above equations, P and S denote the corresponding Peltier and Seebeck effect, σ is the electrical conductivity. The complete description of these parameters is provided in the nomenclature along with their units.

Table 7-1. Material properties in simulation (Comsol version 5.2a, 2016)

Thermoelectric Material	**Bismuth Telluride (Bi_2Te_3)**
The Seebeck Coefficient	210×10^{-6} V/K at 300 K
Electrical Conductivity	$.86957 \times 10^5$ S/m
Thermal Conductivity	1.6 [W/(m*K)]
Dimensions	Varied

Conductor Material	**Copper (Cu)**
Electrical Conductivity	5.998×10^7 S/m
Thermal Conductivity	400 [W/(m*K)]
Dimensions	(1×1×.25) mm
Insulating Substrate Material	**Alumina (Al_2O_3)**
Thermal Conductivity	35 [W/(m*K)]
Electrical Conductivity	0
Modulus of Elasticity	400×10^9 Pa
Dimensions	(24×24×2) mm

TEC 1 was taken as a sample for verification of the Comsol model. The Comsol model of TEC 1 (see Appendix C) was compared with the experiment of TEC 1. The experiment set-up was discussed previously (see Figure 6-5). It is noted that in the test-bed, the heatsink was used for dissipating the heat from the hot side of TEC and it maintained the temperature at the hot side of TEC 1 at 51^{o}C, and this corresponds to the boundary temperature at the hot side of TEC 1 in the Comsol model to be 51^{o}C (more details regarding this note can be found in Appendix C).

The simulation results are shown in Figure 7-1. The comparison of the experimental result (Experiment 1) and the simulation (Simulation 1) result is shown in Table 7-2. In general, the experimental result and the simulation result have a relative error of about 31.80%. The possible reason for the error is the assumptions made in the simulation. In the modeling, the information of the substrate material as well as the thermoelectric material was not provided by the manufacturer but based on the author's estimation (see Appendix C for details). Further, the information of the geometry of TEC 1 was not provided by the manufacturer either but based on the author's measurement (see Appendix C for details). The first source of uncertainty may cause a systematic error of 100% (materials are not known at all) and the second source of uncertainty may cause a systematic error of 33% (confidence level for 2 out of three measurements is above 95%). The

total uncertainty in the experimental result is 33% ((33/100) × (100/100)×100/100 =33/100 =33%), which is larger than 31.80%.

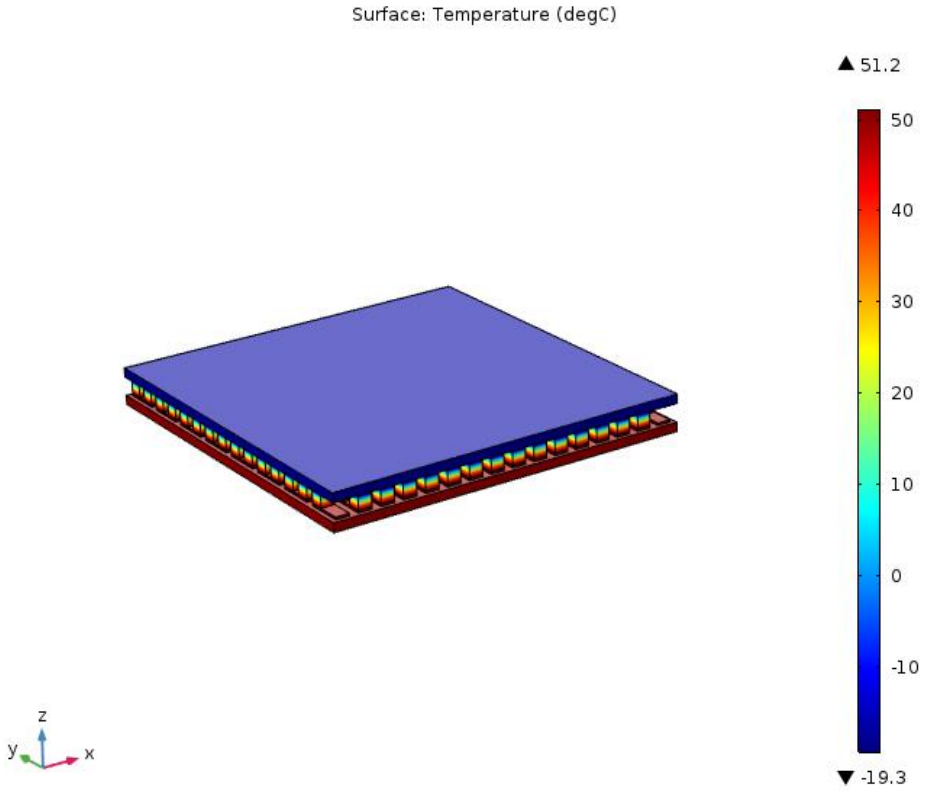

Figure 7-1. Simulation of TEC 1 used in the experiments

Table 7-2. Comparison of the experimental and simulation results for TEC 1

Type of study	**Module(s) and heatsink used**	**Heat Load Q_h (Watts)**	**Cold Side Temperature T_c (ºC)**	**Hot Side Temperature T_h (ºC)**
Experiment 1	TEC 1, Heatsink 1	48	-28.3	51.0
Simulation 1	TEC 1	48	-19.3	51.0

7.2. Design of the Thermoelectric Cooler

The design of TEC has three aspects (Zhao et al., 2014): (1) geometric design (length, cross-sectional area, number of thermocouples), (2) working conditions (Power Input) design, (3)

cooling system design (heat transfer area, thermal resistance). In the following, the three aspects of design are discussed in detail.

7.2.1. Geometric design

Geometric design includes determining thermoelement length (l_e), cross-sectional area (A_e), and number of thermocouples (N). Figure 7-2 shows a thermoelement with its length and area indicated. While determining the geometrical parameters, the type of material is already fixed. This study assumes that the materials were given – see Table 7-1. The design was conducted using the simulation system as developed above. In the following, the optimal determination of these parameters is described.

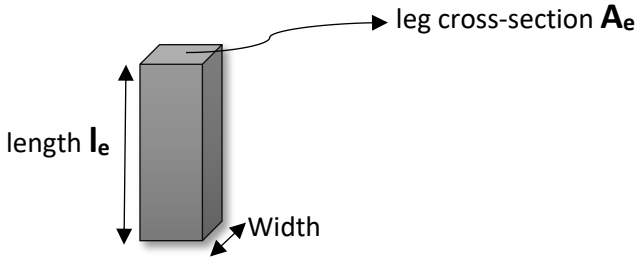

Figure 7-2. A thermoelement

Cold Side Temperature (T_c) vs. Leg-Cross Section (A_e) ('Leg' refers to one thermoelement of Figure 7-2) : In this study, the cross-sectional area of the thermoelements in the thermoelectric cooler from the Comsol application libraries (the procedure in the Comsol interface is: Application Library → Heat Transfer Module → Applications → thermoelectric cooler; where '→' means 'go to') was varied from 0.5×0.5 mm^2 to 1×1 mm^2 and then from 1×1 mm^2 to 1.8×1.8 mm^2 to observe its effect on the cold side temperature. The length of the thermoelectric element was 1.7 mm. The input current I to be 4 A and the temperature of the hot side of the thermoelectric cooler was kept at 323.15 K. Figures 7-3(a) and 7-3(b) show the simulation result. It can be observed from Figure 7-3(a) that the temperature of the cold side gradually drops down with an increase of the leg cross-section and the lowest temperature was achieved at the maximum cross-section value of 1×1 mm^2. With further increase in the area (see Figure 7-3(b)), the temperature drops down further but only until cross-sectional area of 1.2 mm^2 after which it tends to increase. The lowest temperature was achieved at the cross-section value of 1.2×1.2 mm^2, which was taken in the TEC design.

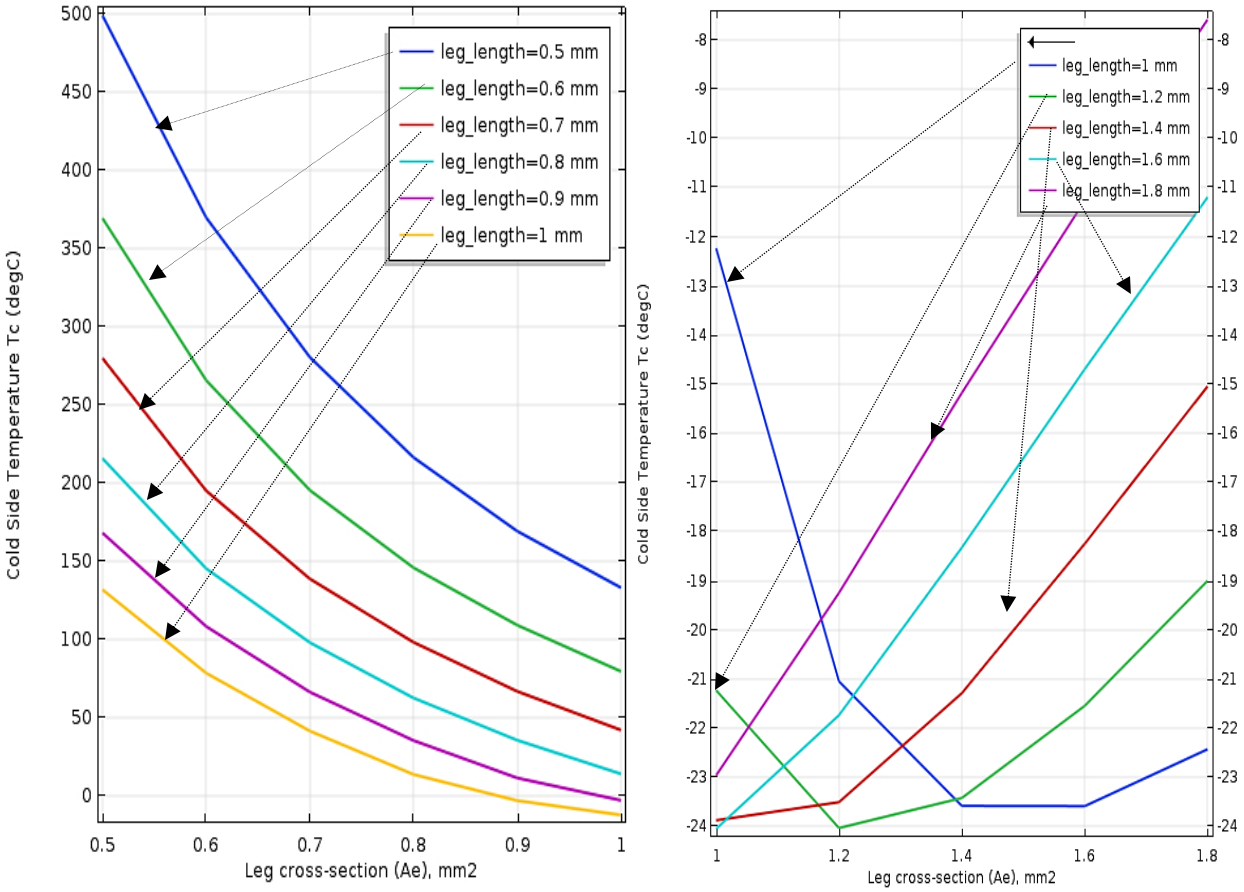

(a) (b)

Figure 7-3. Cold side temperature (T_c) vs. Leg cross-section (A_e)

Cold Side Temperature vs. Length of the Thermoelement: At this point, with the known optimized cross-sectional area, a single stage thermoelectric cooler was modeled in Comsol (see stage 1 in Appendix B), the cross-sectional area of the thermoelements was fixed at 1.2×1.2 mm^2, and the length of the thermoelectric element was varied from 1 to 8 mm to observe its effect on the cold side temperature. The input current I was fixed at 2 A, and the temperature of the hot side of the thermoelectric cooler was kept at 313.13 K. Figure 7-4 shows the simulation result.

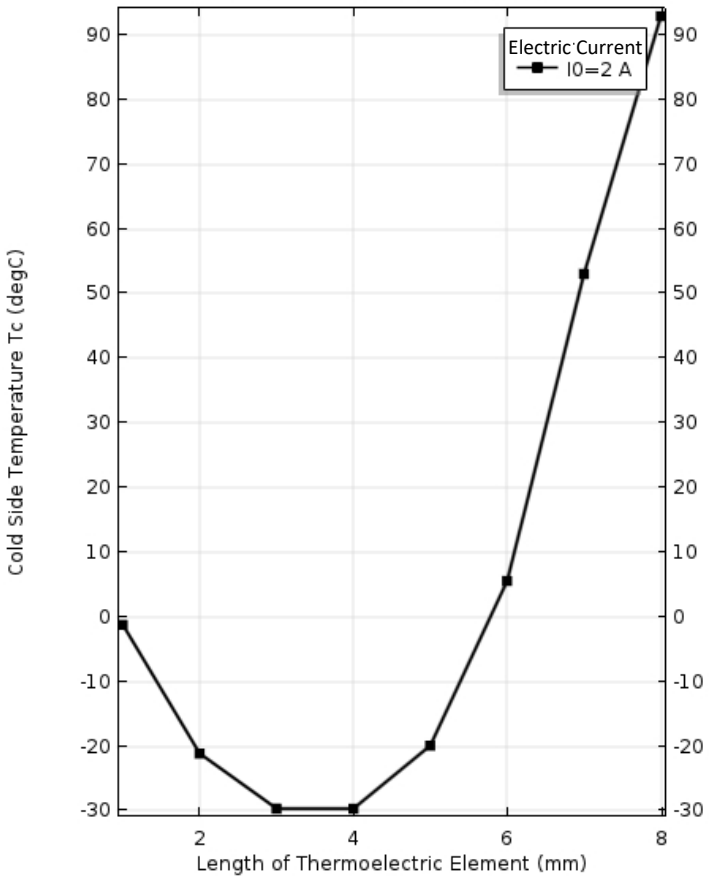

Figure 7-4. Cold side temperature (T_c) vs. leg-length (l_e) at 2 A current

It can be seen from Figure 7-4 that the cold side temperature gradually drops up to a length of 3 and 4 mm and then starts to increase. This phenomenon may be due to the volumetric joule heating that accumulates in the middle of the thermoelement as heat flow in the thermoelement is proportional to thermal conductance (Equation 3.7 and Equation 3.14) which decreases with increase in length (K=kA/L). Figure 7-5(a) illustrates this phenomenon graphically with a thermoelement length of 8 mm. This cooler does not have a uniform temperature distribution from hot side to cold side, but the temperature is higher in the middle of thermoelements. Figure 7-5(b) shows the same single stage thermoelectric cooler with an optimized thermoelement length of 4mm. It should be noted that for a given number of thermoelements in a thermoelectric cooler, which are electrically connected in series and thermally connected in parallel, the flow of heat is only along the length of the thermoelement (i.e., one-dimensional heat transfer). If a horizontal plane cuts these elements perpendicular to the direction of length, all the elements on the plane will have isothermal contours.

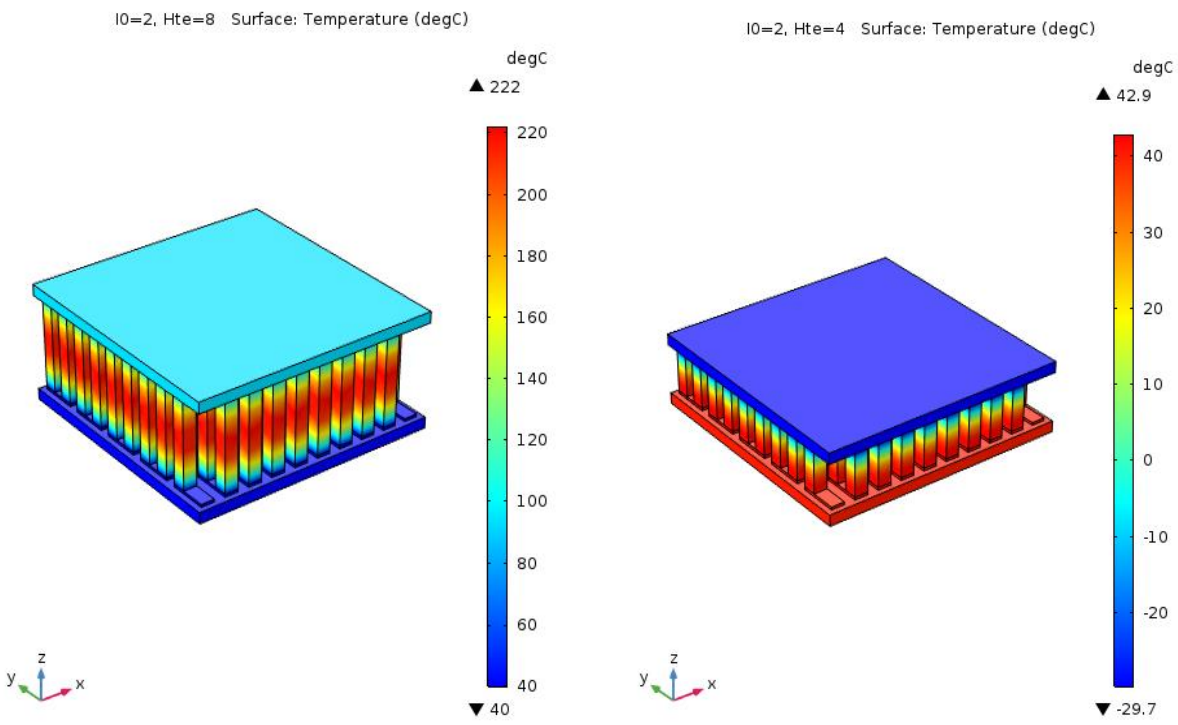

(a) (b)

Figure 7-5. Effect of Joule heating and optimized length of the element (Temperature in ℃)

7.2.2. Working Condition Design

Effect of Boundary Conditions: The environment in which a thermoelectric cooling system works has an impact on the overall performance of the thermoelectric cooling system. A thermoelectric cooling system is designed for a suitable temperature range and using it beyond this range may result in the total failure of the system. There are many reasons for a system to fail: (1) the solder temperature is lower than the operating temperature, (2) the hot side temperature may result in heating up the cold side, and (3) the condensation from the environment can degrade the performance.

Effect of Different Ceramic Substrates: The purpose of the substrate is to provide electrical insulation from the conducting thermoelements and to strengthen the structure. A good substrate must have high thermal conductivity and should be an electrical insulator. It should possess a good material strength as well.

Input Power: Input power is an important parameter that affects the performance of the thermoelectric cooling system. An increase in input power will increase the temperature difference, yet due to the increase in irreversible joule heating ($\boldsymbol{I^2R}$) more heat needs to be removed at the hot side. Therefore, optimization of input power is very important. The goal is to maximize the temperature difference while minimizing joule heating. A parameter variation analysis was conducted in this study to determine the optimal input power. The result of this analysis is shown in Figure 7-6, where one can find the length of the thermoelectric element was varied from 1 to 8 mm and the input current from 1 to 8 A. It can be found from Figure 7-6 that the temperature first drops down and then increases gradually. However, at higher currents, this change is more abrupt, suggesting that current should be kept as low as possible to avoid the volumetric joule heating ($\boldsymbol{I^2R}$).

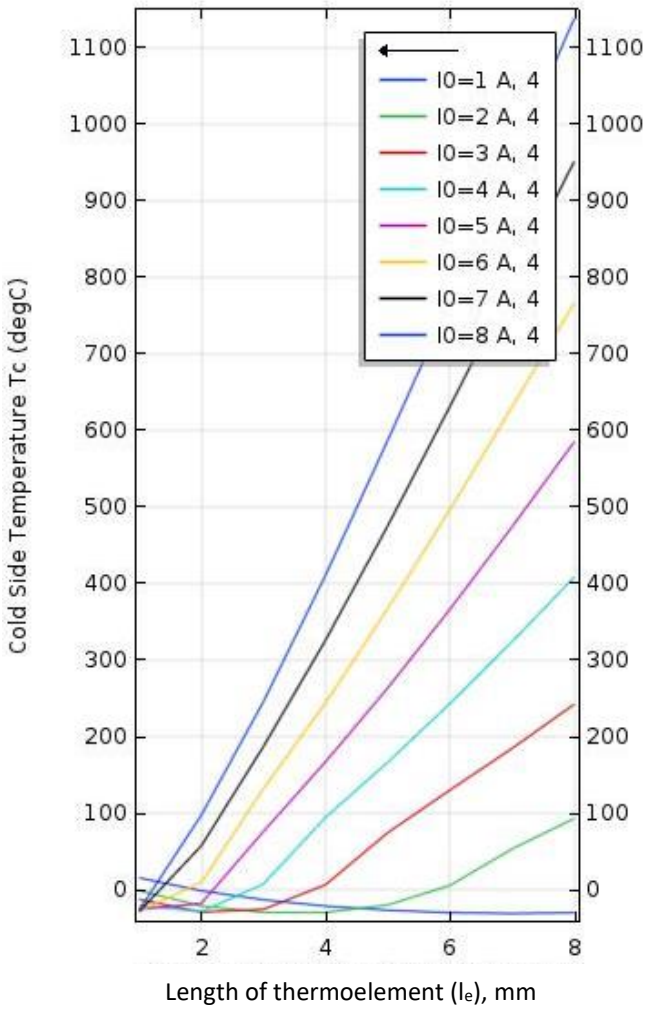

Figure 7-6. Cold side temperature T_c vs. length of thermoelement (l_e) at various currents (I)

7.2.3. Cooling System Design

The so-called cooling system design here refers to designing the heatsink system to dissipate heat from the hot side of TEC. This is only possible if a cooling system or heatsink is specific to a TEC in a specific application. While there are many cooling systems available (see Chapter 5), each application will require its own heatsink depending upon the heat load, ambient conditions, and constraint on the volume of the system.

A specific heatsink system, which is also called vapor chamber, designed in this study will be presented in Section 7.5. But first, the design of an application customized cooler along with its verification is discussed in the following, Section 7.3, and Section 7.4, respectively.

7.3. Design of the Cascaded Cooler

For dental pulp testing, the thermoelectric cooler needs to provide a stable cryogenic temperature of -60℃, and that is not possible to achieve by a single stage thermoelectric cooler according to the study presented in section 7.2.

A cascaded cooler was designed with the help of the Comsol simulation system. Particularly, the cascaded cooler consists of two stages with Stage 2 on the top of Stage 1. Stage 1 utilized the optimal parameters and optimal input current from the results of the study presented in Section 7.2, while Stage 2 was modeled in the context that is it is on the top of Stage 1 (see Appendix B for a detailed model). Stage 2 (or the upper stage) used the same materials as Stage 1 presented in Table 7-2. It also used the same cross-section of thermoelements, but the length was varied to find the optimal one.

To find the optimal length of thermoelements of Stage 2, the temperature at the cold side of Stage 2 was examined at various electric currents as a function of the length of the thermoelement, as shown in Figure 7-7. From Figure 7-7 it can be seen that the lowest temperature at the cold side was obtained at the thermoelement length of 3 mm and with the current input of 2 A.

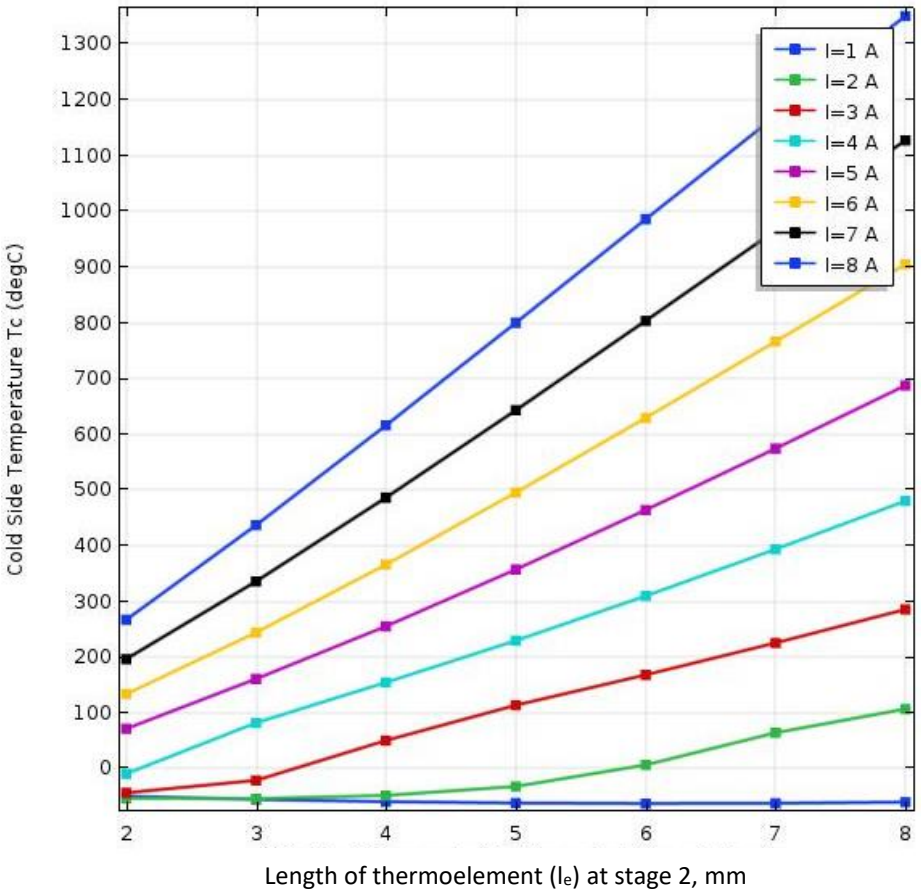

Figure 7-7. Cold side temperature T_c vs. length of thermoelement (l_e) at various currents (I) for Stage two or the upper stage

The simulation was then performed to optimize Stage 1 (or the lower stage) in the context that there is an upper stage. The significance of finding the optimal parameters for Stage 1 lies in the fact that for a cascaded thermoelectric cooler, a lower stage acts as a heatsink for an upper stage. Therefore, the heat load to the lower stage changes with the changing parameters of the upper stage, because the lower stage needs to dissipate heat coming out from the hot side of the upper stage. With this heat load coming into the lower stage from the upper stage that is known after the design of the upper stage is done, the length of the thermoelement and input current for Stage 1 (lower stage) needs to be determined. It is worth mentioning that design at this point refers to the determination of the geometry of the thermoelement (Figure 7-2). To find the optimal length of the thermoelement at Stage 1, the temperature at the cold side of Stage 2 was examined at various currents as a function of the length of the thermoelement in Stage 1, and the result is shown in Figure 7-8.

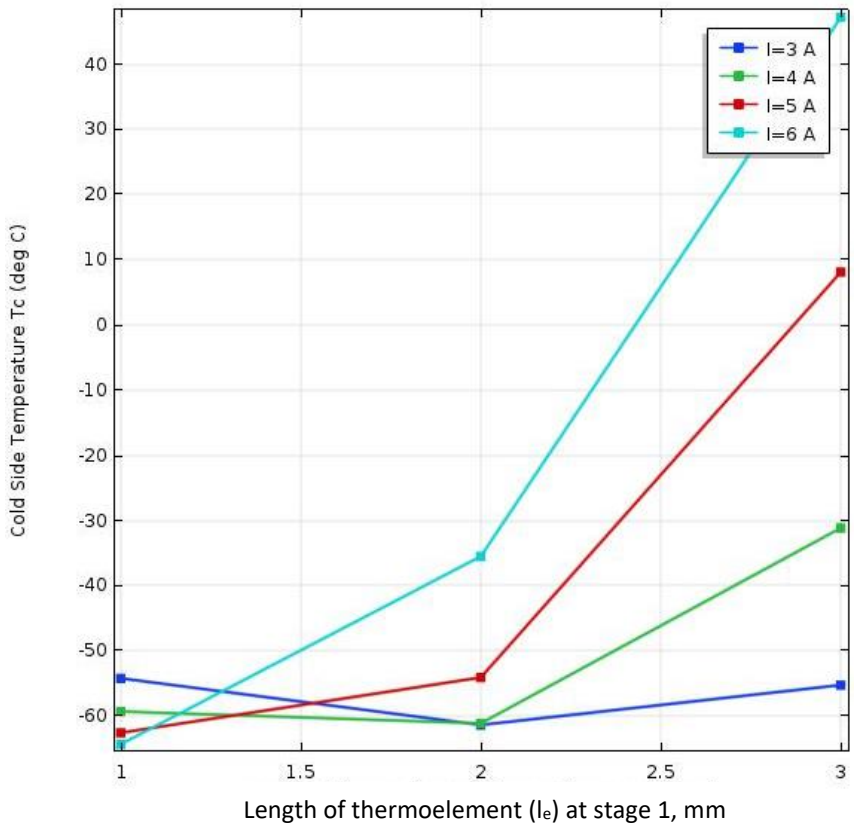

Figure 7-8. Cold side temperature T_c vs. length of thermoelement (l_e) at various currents (I) for Stage 1 or the lower stage

The new optimal parameters for the thermoelement length and current for Stage 1 (or the lower stage) are 2 mm and 3 A, respectively as compared to previously optimized parameters of 4mm and 2 A.

The final design of the cascaded thermoelectric cooler for the dental pulp testing device with all these optimal parameters, as discussed in Section 7.2 and Section 7.3, is shown in Figure 7-9 (the complete Comsol model for simulation is presented in Appendix B). The lowest temperature at the cold side of the cascaded cooler is -61.7℃.

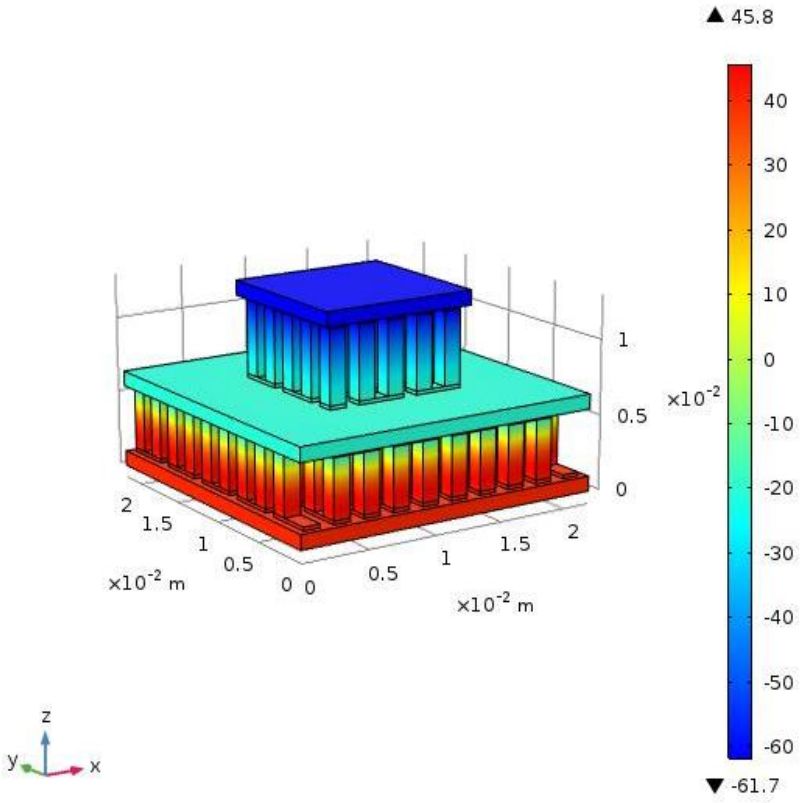

Figure 7-9. Cascaded thermoelectric cooler for the dental pulp testing device

7.4. Model Verification of the Cascaded Thermoelectric Cooler

The model verification of the thermoelectric cooler was performed with an energy equilibrium model which is an analytical formula. This formula is expressed as (Zhao et al., 2014):

$$\dot{Q}_c = \alpha T_c I - \frac{1}{2} I^2 R - K (T_h - T_c) \qquad (7.12)$$

where

- $\dot{Q}_c$ = 2.13 Watts (Input power to the upper stage),
- α= 210 µV/K,
- **I**= 3 A,
- **k**= 1.6 $Wm^{-1}K^{-1}$,
- **R**= .02 Ω, and
- T_h = 313.15 K.

The material properties **α**, k, and the input parameters Q_c, I, and T_h are the same as used in the simulation (see Appendix D). R is the resistance of thermoelements, and it is fixed for a given geometry.

The idea was to consider this formula as a reference model and to compare the Comsol model with the reference model on the information of some parameters (e.g., temperature). The model verification approach was applied to Stage 1 (or the lower stage). From Equation (7-12), $\mathbf{T_c}$ = 240 K or -33.3℃. From the Comsol model, $\mathbf{T_c}$ = 245 K or -28℃. The difference in the two models was around 5 K, and the possible reason is the assumptions made in both models that ignore some factors (e.g., the passive loads and condensation from the ambient air). A sensitivity analysis for the theoretical model was performed for the input parameters Q_c, I, and T_h (**α**, k, and R remain the same for the given set of materials and geometry) to observe the robustness of the design with respect to these parameters and the result is summarized in Figure 7-10 (see Appendix B for details).

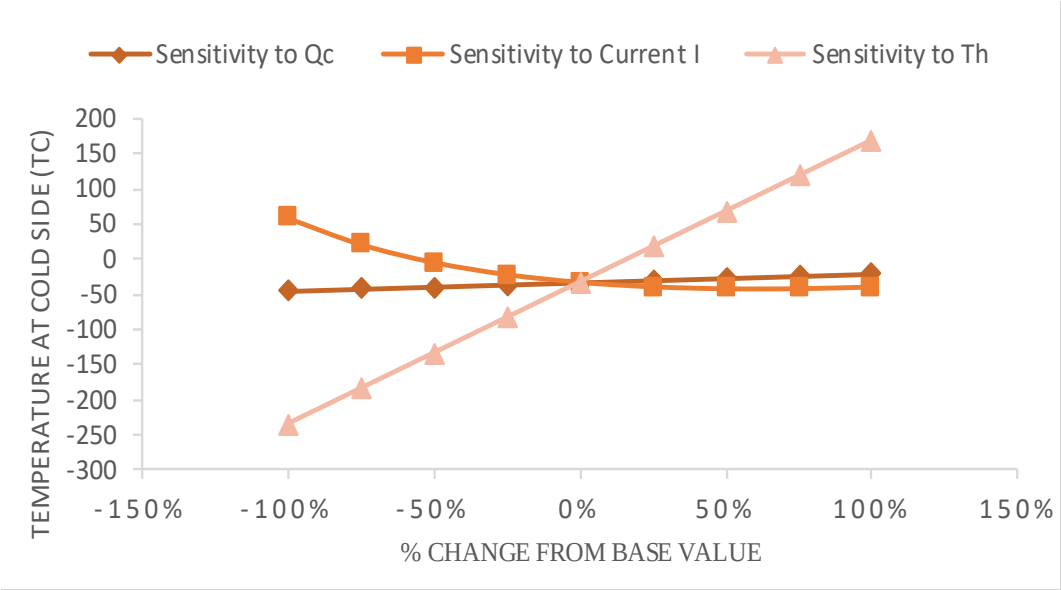

Figure 7-10. Sensitivity analysis of the theoretical model

It can be observed from the analysis that the system is most sensitive towards the temperature at the hot side. This sensitivity analysis was also performed for the simulation model. To minimize the computational cost, only T_h (i.e., the temperature at the hot side) was selected. The result of the analysis is presented in Figure 7-11 along with the corresponding theoretical model. The

simulation model shows the same pattern of sensitivity with respect to the temperature at the hot side.

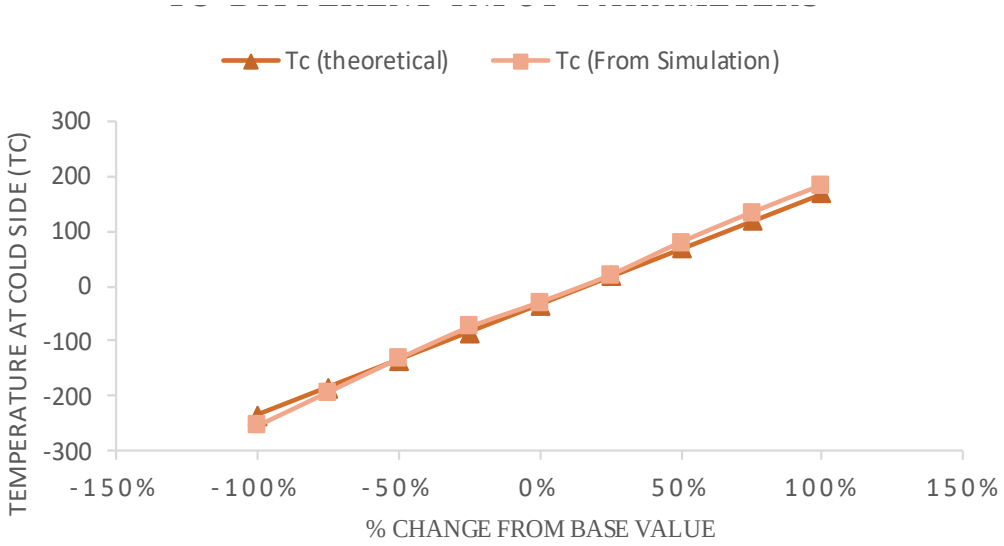

Figure 7-11. Sensitivity analysis of the simulation model for T_h

7.5. Design of the Vapor Chamber

The goal of the design of the vapor chamber was to maintain the temperature at the hot side of the cascade cooler to be below 40℃. Comsol was used to model the vapor chamber which includes the thermal conductivity of the vapor core in the chamber. The design utilized the Comsol developer model of the flat heat pipe model. The simulation was performed to design the vapor chamber to meet the requirements as follows:

- It can dissipate up to 30 Watts of heat from the thermoelectric cooler (approx. 22 Watts was the power consumed by the proposed cascaded thermoelectric cooler),
- It can maintain the hot side temperature of TEC below 40℃, and
- It should fulfill the dimensional criteria of the pulp testing device.

Some parameters of the vapor chamber are:

- Dimensions: (30×60×5) mm,
- Material(s): Aluminum, Water, and
- Heat load: 30 Watts.

The maximum temperature of the vapor chamber is at the interface of the hot side of the thermoelectric cooler and the vapor chamber (see Figure 7-12). The temperature is uniformly distributed across the length, width, and height of the vapor chamber (i.e. heat transfer in 3D) because of its high thermal conductivity and hence more heat conduction capability in all the directions.

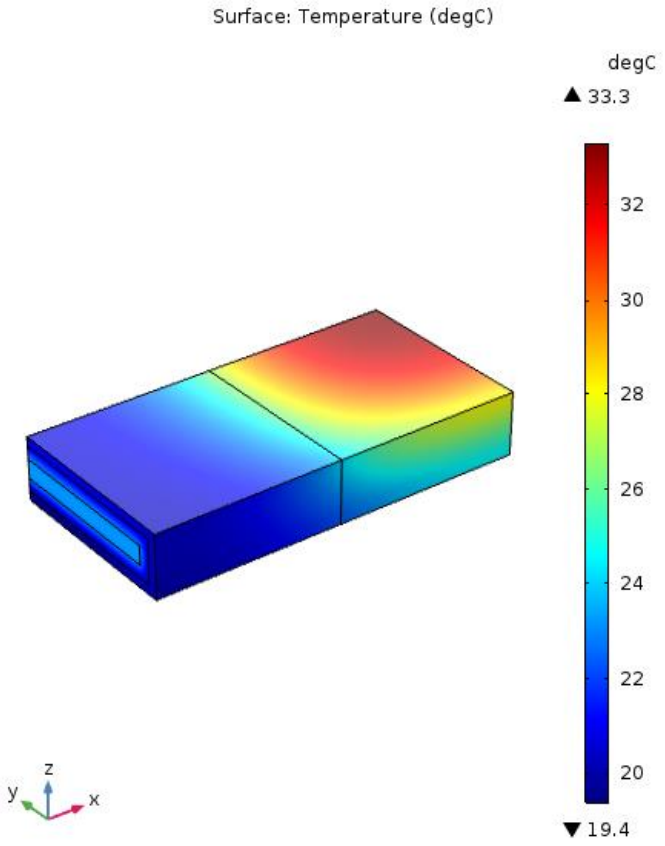

Figure 7-12. Comsol model of the vapor chamber for the proposed thermoelectric cooling system

7.6. Experimental Validation of the Vapor Chamber

The design of vapor chamber needs to be validated for its effectiveness. The validation approach taken in this study was to make use of a heatsink that is close to the designed vapor chamber. It is noted that the heatsink and vapor chamber are just two different names for the same thing – that is a system that dissipates the heat at the hot side of a cooler. In the validation process, the cooler system is the TEC 2 as described in Section 6.1.1 and the heatsink (Figure 7-13) is the off-the-shelf Aluminum vapor chamber. Figure 7-14 shows the entire physical system in the experiment: TEC 2 and the heatsink 2. The specifications of the heatsink 2 are shown in Table 7-3. The heatsink

2(80×30×5) is not as per design with the difference of 20 mm in length from the designed one (60×30×5) while the other dimensions, as well as the materials, are the same. Modeling of the vapor chamber or heatsink for both lengths (60, 80) with Comsol was performed.

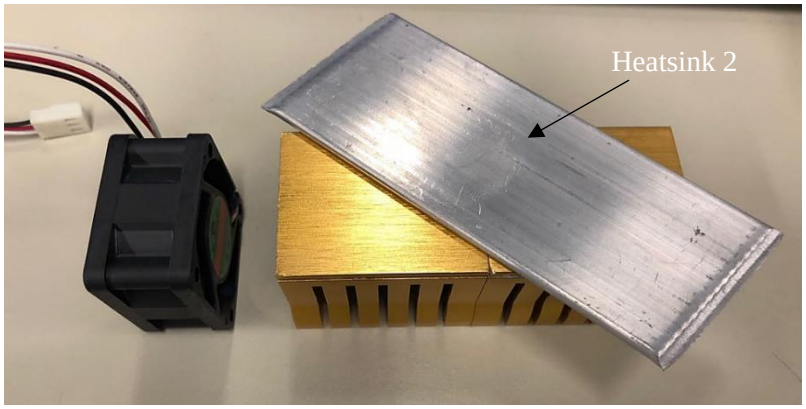

Figure 7-13. The heatsink 2 (vapor chamber) used for the experimental validation of the design

Table 7-3. Properties of the heatsink 2

Type of phase change mechanism	The aluminum flat vapor chamber
Fin Material	Aluminum pin fin
Fan Speed	900 RPM
Dimensions	80(L) × 30(W) × 5(H)mm
Weight	120 g

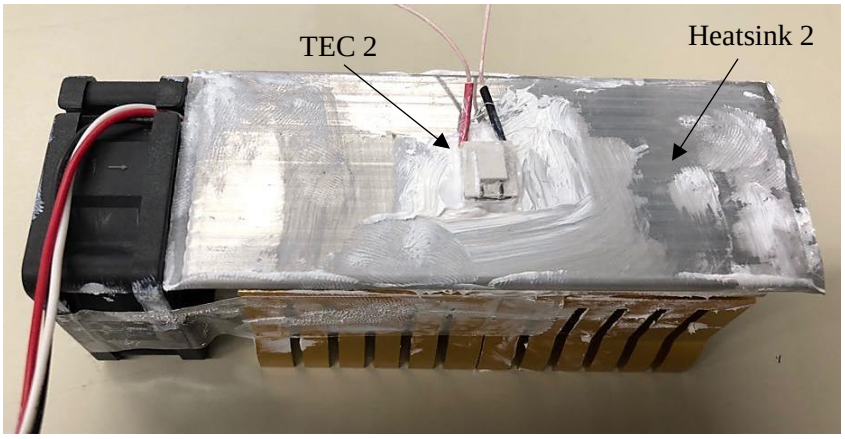

Figure 7-14. The heatsink 2 and TEC for the experimental validation of the design

The experimental result along with the Comsol simulation is shown in Table 7-4. It is noted that in the experiment, the heatsink 1 was also tested and its result is listed in Table 7-4 as well. The IR thermal image of Experiment 4 is shown in Figure 7-15. The temperature profile shows that the heat is evenly distributed on the vapor chamber. It is interesting to observe that the heatsink 2, which is smaller in size than the heatsink 1, can achieve a larger temperature difference than the heatsink 1 does for TEC 2.

Table 7-4. Comparison of the results

No.	**Module(s) and heatsink used**	**Heat Load Q_h (Watts)**	**Cold Side Temperature T_c (ºC)**	**Hot Side Temperature T_h (ºC)**
Experiment 2	TEC 2, Heatsink 1	3.81	-32.5	23.5
Comsol Model 1	Designed Vapor Chamber (L=60mm)	30	N/A	33.3
Comsol Model 2	Designed Vapor Chamber (L=80mm)	30	N/A	30.4
Experiment 4	TEC 2, Heatsink 2	3.81	-33.1	24.8

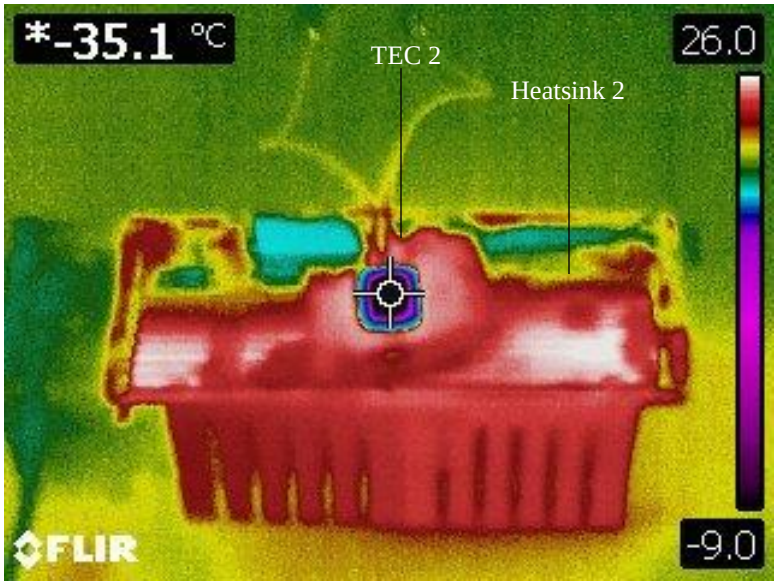

Figure 7-15. IR thermal image of the Vapor chamber and TEC in the steady state operation

Figures 7-16. (a) and (b) show the temperature at the heatsink and close to the hot side of TEC, which is about 25℃, suggesting the effectiveness of the vapor chamber heatsink.

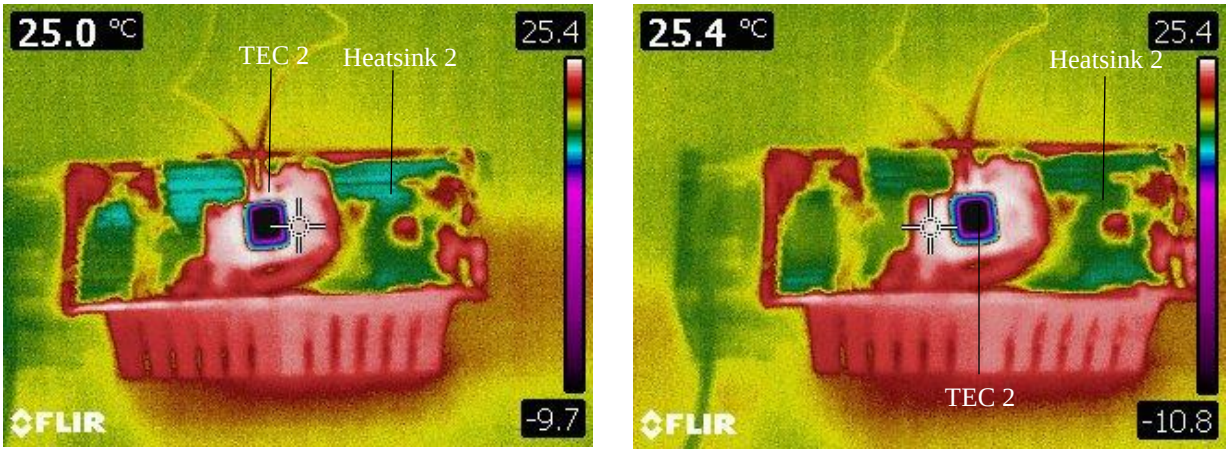

(a) (b)

Figure 7-16. The temperature at the interface of the heatsink and TEC

7.7. Conclusion

A cascaded thermoelectric cooler was designed and further modeled with Comsol Multiphysics, and then optimized in such a way that it can achieve -60℃ at its cold side while utilizing a minimum current. The significance of the minimum current is that the cooler will reject a low amount of heat and the temperature at the hot side of the cooler will not increase beyond the acceptable limits (i.e., 40℃, see Section 7.2.2). From the simulation results, it can be concluded that an optimized cascaded thermoelectric cooler can achieve a temperature of -60℃ at its cold side for a pulp testing device provided that the temperature at the hot side remains 40℃ or below. Furthermore, a vapor chamber can effectively maintain the temperature at the hot side of TEC below 40℃ (33.3℃ precisely, see Table 7-4) because of its effective thermal conductivity. The validation of the thermoelectric cooler and vapor chamber, as designed, supports the design.

Chapter 8

Conclusion and Future Work

8.1. Overview and conclusions

The overall objective of this thesis study was to synthesize a solution for dental pulp testing and to design a device that is portable, reliable, and safe in use. The specific objectives of the study are revisited herein.

Specific Objective 1: *To verify the feasibility of the thermoelectric cooling principle of the device to achieve the requirement for dental pulp testing*.

Specific Objective 2: *To develop a simulation system for the device for dental pulp testing*. The simulation system is needed to optimize the design of the device.

Specific Objective 3: *To construct a proof-of-concept prototype of the device for dental pulp testing.* The prototype is needed to test the proposed device against the requirement of the device.

The specific objectives have been achieved. Particularly, thermoelectric cooling technique was explored for the dental pulp testing device to achieve -60℃ at the probe while keeping the device portable and stand-alone.

Testing was conducted with the off-the-shelf thermoelectric coolers to see if they can achieve the requirements. After the promising results were achieved from the experiment, a thermoelectric cooler was designed and optimized for dental pulp testing. This thermoelectric cooler can achieve - 60℃ as shown by simulations, provided that the hot side temperature of the thermoelectric cooler is kept below 40℃. This condition can be met by designing a heatsink which can dissipate up to 30 Watts of heat produced at the hot side of the designed thermoelectric cooler. A validation based on the energy balance equation was employed to verify the designed cascaded thermoelectric cooler.

The conclusions from the study are presented below:

(1) The phase change cooling in the form of heat pipes could effectively maintain the temperature in the desired range, i.e., below 40℃.

(2) The heatsink embedded with heat pipes used in the experiment was too large to allow portability of the pulp testing device.

(3) The application customized and optimized thermoelectric cooler can achieve - 60℃ at its cold side which was the set target for this study.

(4) The temperature at the hot side of the TEC can be maintained below 40℃.

The final design of the device is shown in Figure 8-1. The device is compact with the envelope of $30 \times 30 \times 120$ mm^3, containing the cooler, vapor chamber and battery, and it allows for portability. It will not require any inlet or outlet for the circulation of the cooling liquid, and thus it is ready for stand-alone application in pulp testing. Due to the limited resources and time available, a prototype closet to the actual device could not be built in this thesis.

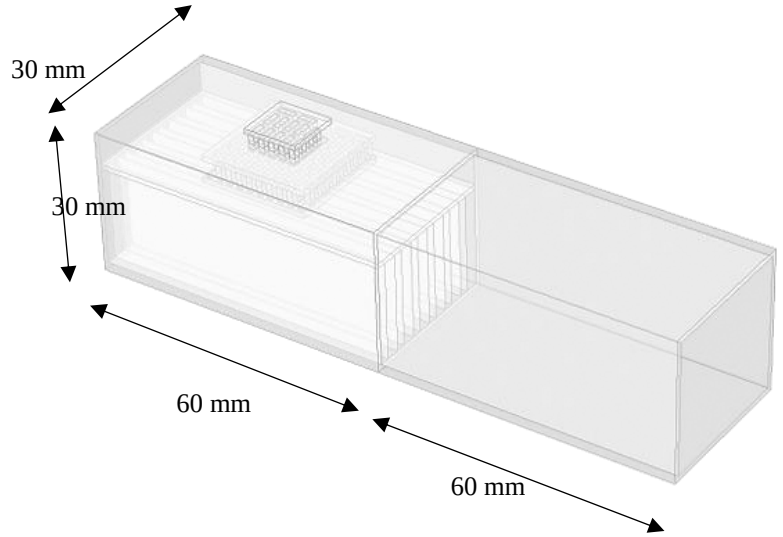

Figure. 8-1. Conceptual Design of the Thermoelectric Dental Pulp Testing Device

8.2. Contributions

The following contributions are made by this study:

(1) In the clinic application, this study has provided a highly feasible solution to a stand-alone, portable and stable temperature (up to -60 ^{o}C) dental pulp testing device. Since the device is based on the TEC principle, it is possible to control the prescribed temperature overall within a prescribed range, thus allowing personalized testing for an improved

precise diagnosis of dental diseases. It is noted that in current clinic practice, precise control of the temperature over a duration is not possible.

(2) This study has provided a step-by-step guide for the design of cascaded thermoelectric coolers with the Comsol model. This may have a generalized implication to other similar device development.

8.3. Future Work

The current study explored the thermoelectric cooling technique for dental pulp testing. However, there are many other fields of medicine and surgery, which require cold temperatures or where cryogenic temperatures can help achieve the required treatment process. Thermal ablation of cancerous cells is an example. A similar device may be constructed, which will cool down the needle or probe used for this treatment process.

The work from this study can be taken further to the fabrication of a microdevice with MEMS-based thermoelectric coolers and a vapor chamber to investigate whether the temperature could be achieved at the microdevice level. With the trend of the decreasing size in electronics, miniaturized heatsinks are the need of the hour. The cooling system for electronics cooling may be designed using thermoelectric coolers and vapor chamber heat spreaders.

References

Anandan, Sundaram, and Ramalingam, V. (2008). Thermal management of electronics: A review of literature. *Thermal Science* 12, no. 2: 5-26. doi:10.2298/tsci0802005a.

Abd-Elmeguid, A., and Donald, C. Yu. (2009). Dental Pulp Neurophysiology: Part 2. Current Diagnostic Tests to Assess Pulp Vitality," *Journal of Canadian Dental Association*, Vol. 75, No.1.

Blausen.com staff. (2014). Medical gallery of Blausen Medical 2014. *WikiJournal of Medicine* 1 (2): 10. doi:10.15347/wjm/2014.010. ISSN 2002-4436.

Blazej, D. (2016). Thermal Interface Materials. Electronics Cooling. October 20, 2016. Accessed March 15, 2018. https://www.electronics-cooling.com/2003/11/thermal-interface-materials/.

Brown, R. W. (1972). Dental Pulp Tester. U.S. Patent 3,782,366 filed Mar. 16, 1972, and issued Jan. 1, 1974.

Brown, D., Bulmer, J., Gadzella, T., and Trent, S. (2016). Design of a dental pulp stimulator. Mechanical Engineering Capstone Project. University of Saskatchewan.

Chen, A., and Wright, P. (2012). Medical Applications of Thermoelectrics. In *Modules, Systems, and Applications in Thermoelectrics*, edited by David M Rowe, 26-1. CRC Press DOI: 10.1201/b11892-30

Chen, E., and Abbott, P. (2009). Dental Pulp Testing: A Review. *International Journal of Dentistry*, Article ID 365785 (doi:10.1155/2009/365785)

Chen, X., Ye, H., Fan, X., Ren, T., and Zhang, G. (2015). A review of small heat pipes for electronics. *Applied Thermal Engineering*. http://dx.doi.org/doi: 10.1016/j.applthermaleng.2015.11.048.

Davis, L. B. (1981). Dental Pulp Tester. U.S. Patent 4,350,488 filed Jun. 29, 1981, and issued Sep. 21, 1982.

Dresselhaus, Mildred, S., Chen, G., Tang, M., Yang, R., Lee, H., Wang, D., Ren, Z., Fleurial, J., and Gogna, P. (2007). New Directions for Low-Dimensional Thermoelectric Materials. *ChemInform*38, no. 26. doi:10.1002/chin.200726202.

Dummer, P. M., Hicks, R., and Huws, D. (1980). Clinical signs and symptoms in pulp disease. *International Endodontic Journal*, vol. 13, no. 1, pp. 27–35.

Ehrmann, H. (1977). Pulp testers and pulp testing with particular reference to the use of dry ice. *Australian Dental Journal*, vol. 22, no. 4, pp. 272–279.

Eidus, W. (1962). Thermoelectric Medical Instrument. U.S. Patent 3,133,539 filed Aug. 6, 1962, and issued May 19, 1964.

Electrical4u. n.d. Seebeck Effect and Seebeck Coefficient. Accessed June 13, 2016. https://www.electrical4u.com/seebeck-effect-and-seebeck-coefficient/.

Fan, L.X., Cai, M.Y., Lin, Y., and Zhang, W.J. (2015). Axiomatic Design Theory: further notes and its guideline to applications. *International Journal of Material and Product Technology (IJMPT)*. 51(4), pp. 359–374.

Ferrotec Nord Corporation n.d. Advantages of Thermoelectric Cooling. Accessed December 12, 2016. http://www.ferrotec-nord.com/technology/intro-thermoelectric-cooling/advantages-thermoelectric-cooling.

FerroTec Thermal Management Solutions n.d. Intro to Thermoelectric Cooling. Accessed June 13, 2016. https://thermal.ferrotec.com/technology/thermoelectric-reference-guide/thermalref01/.

Frank, U., Freundlich, J., Tansy, M. F., Chaffee Jr., Weiss, R. C., and Kendall, F. M. (1972). Vascular and cellular responses of teeth after localized controlled cooling. *Cryobiology*, vol. 9, no. 6, pp. 526–533.

Heat Transfer Module, COMSOL Multiphysics® v. 5.2a. (2016). COMSOL AB, Stockholm, Sweden.

Jespersen, J., Hellstein, J., Williamson, A., Johnson, T., and Qian, F. (2014). Evaluation of Dental Pulp Sensibility Tests in a Clinical Setting. *Journal of Endodontics*, Vol. 40, No. 3.

Lee, H. (2010). *Thermal Design: Heat Sinks, Thermoelectrics, Heat Pipes, Compact Heat Exchangers, and Solar Cells*. Hobooken: John Wiley & Sons, Inc.

Major, E. (1981). Thermoelectric Diagnostic Instrument. U.S. Patent 4,308,013 filed Jun. 19, 1980, and issued Dec. 29, 1981.

Mejia, Natalia, Dedow, K., Nguy, L., Sullivan, P., Khoshnevis, S., and Diller, K. R. (2015). An On-Site Thermoelectric Cooling Device for Cryotherapy and Control of Skin Blood Flow. *Journal of Medical Devices* 9, no. 4. doi:10.1115/1.4029508.

Milner, R., and Doherty, C. (2015). Pathophysiology of Pain in the Peripheral Nervous System. *Nerves and Nerve Injuries,*3-22. doi:10.1016/b978-0-12-802653-3.00050-6

Mumford, J. (1964). Evaluation of gutta-percha and ethyl chloride in pulp testing. *British Dental Journal*, vol. 116, pp. 338–342.

Napeñas, J. J. (2013). Intraoral Pain Disorders. *Dental Clinics of North America* 57, no. 3: 429-47. doi:10.1016/j.cden.2013.04.004.

Office of Nuclear Energy. 2013. Role of Modeling and Simulation in Scientific Discovery. Energy.gov. Accessed November 19, 2017. https://www.energy.gov/ne/articles/role-modeling-and-simulation-scientific-discovery.

Peters, D., Lorton, L., Mader, C., Augsburger, R., and Ingram, T. (1986). Evaluation of the effects of carbon dioxide used as a pulpal test—I: in vitro effect on human enamel. *Journal of Endodontics*, vol. 9, no. 6, pp. 219–227.

Petersson, K., Soderstrom, C., Kiani-Anaraki, M., and Levy, G. (1999). Evaluation of the ability of thermal and electrical tests to register pulp vitality. *Dental Traumatology*, vol. 15, no. 3 (1999), pp. 127–131.

Pierce, A. (1998). Pulpal injury: pathology, diagnosis and periodontal reactions. *Australian Endodontic Journal*, vol. 24, no. 2(1998), pp. 60–65.

Ross, R. G. (1999). Continuous use Orthodontic Cooling Appliance. U.S. Patent US 6,196,839 B1 filed Jan. 29, 1999, and issued March 6, 2001.

Scher, J. M. (1966). Diagnostic Instrument used in Testing Patient Response to Heat, Cold and Electrical Stimuli. U.S. Patent 3,533,397 filed May 4, 1966, and issued Oct 13, 1976.

Trowbridge, R., Baker, J., Fuss, Z., and Bender. (1988). Effects of thermal vitality tests on human dental pulp. *Journal of Endodontics*, vol. 14, no. 10(1988), pp. 482–485.

Watson, S. n.d. Tooth Pulp Is the Vital, Living Aspects of Teeth. Verywell. Accessed December 19, 2017. https://www.verywell.com/tooth-pulp-dental-terms-1059180.

Weibel, J. A. and Garimella, S V. (2013). Recent Advances in Vapor Chamber Transport Characterization for High Heat Flux Applications. *CTRC Research Publications.* Paper 228. http://dx.doi.org/http://dx.doi.org/10.1016/B978-0-12-407819-2.00004-9

Yarmolenko, P. S., Moon, E. J., Landon, C., Manzoor, A., Hochman, D. W., Viglianti, B. L., & Dewhirst, M. W. (2011). Thresholds for thermal damage to normal tissues: An update. *International Journal of Hyperthermia : The Official Journal of European Society for Hyperthermic Oncology, North American Hyperthermia Group*, *27*(4), 320–343. http://doi.org/10.3109/02656736.2010.534527

Zach, L. (1972). Pulp lability and repair; effect of restorative procedures. *Oral Surgery, Oral Medicine, Oral Pathology*, vol. 33, no. 1, pp. 111–121.

Zhao, Dongliang, and Tan, G. (2014). A review of thermoelectric cooling: Materials, modeling and applications. *Applied Thermal Engineering* 66, no. 1-2: 15-24. doi:10.1016/j.applthermaleng.2014.01.074.

Appendix A: Uncertainty in Measurement

Systematic Uncertainty

Systematic error calculation for all the measuring instruments used is given below:

- Thermocouple: $\pm$ 0.35℃ =.35/$\sqrt{3}$ (Assuming normal distribution) = 0.20℃ at a confidence level of 99%.
- Multimeter for voltage: $\pm$ 0.1 V =100 mV=100/$\sqrt{3}$ (Assuming normal distribution) =57.75 mV at a confidence level of 99%.
- Multimeter for current: $\pm$ 0.75 A =75 mA=75/$\sqrt{3}$ (Assuming normal distribution) =43.3 mA at a confidence level of 99%.

Total Uncertainty

The total uncertainty consists of the random uncertainty as well as the systematic uncertainty. The systematic uncertainty was calculated above. For the random uncertainty, a statistical tool (i.e., standard deviation calculation) was employed, and the total uncertainty was calculated by

$$Ut = \sqrt{u_r^2 + u_s^2} \quad \textbf{(A.1)}$$

Where u_r is the total random uncertainty and u_s is the total systematic uncertainty. Table A-1 shows the result of the uncertainty analysis for the experiments conducted in this study.

Table A-1. Uncertainty measurement

	Experiment 1		Experiment 2		Experiment 3		Experiment 4	
	Tc (℃)	Th (℃)	Tc (℃)	Tc (℃)	Th (℃)	Th (℃)	Tc (℃)	Th (℃)
1	-26.9	49.3	-31.3	-58.2	58.3	24.5	-35.5	23.7
2	-27.6	47.5	-32.2	-53.8	47.8	22.6	-33.6	22.9
3	-28.8	51.3	-33.4	-56.8	55.6	23.2	-31.7	26.6
4	-29.7	50.2	-30.9	-57.9	51.5	24.3	-34.3	25.3
5	-28.5	56.5	-34.7	-55.8	51.8	22.9	-30.4	25.5
Mean	-28.3	50.96	-32.5	-56.5	53	23.5	-33.1	24.8

Standard Deviation	0.97	3.04	1.40	1.60	3.62	0.76	1.83	1.33
Standard Error	0.43	1.36	0.62	0.71	1.62	0.34	0.82	0.60
Systematic Error	.20	.20	.20	.20	.20	.20	.20	.20
Total Uncertainty	0.47	1.37	.65	.74	1.63	.39	.844	.63

The Error bar analysis is an effective way to show the uncertainty, and it is presented for the experiments in the following figures, showing the total measurement uncertainty of all the experiments conducted in this study (Figure A-1 to Figure A-4).

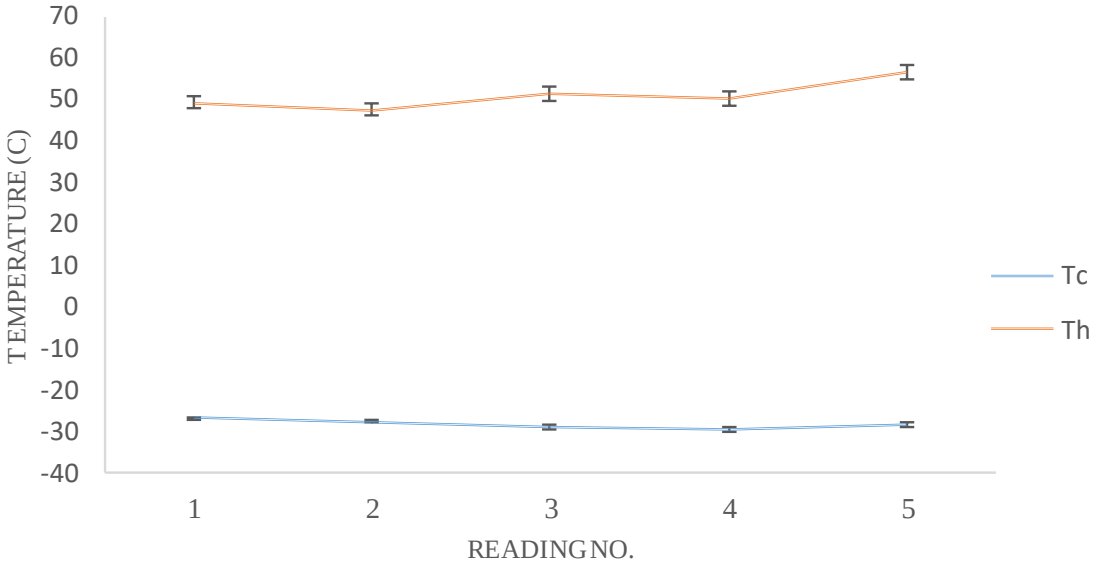

Figure A-1. Measurement uncertainty in experiment 1

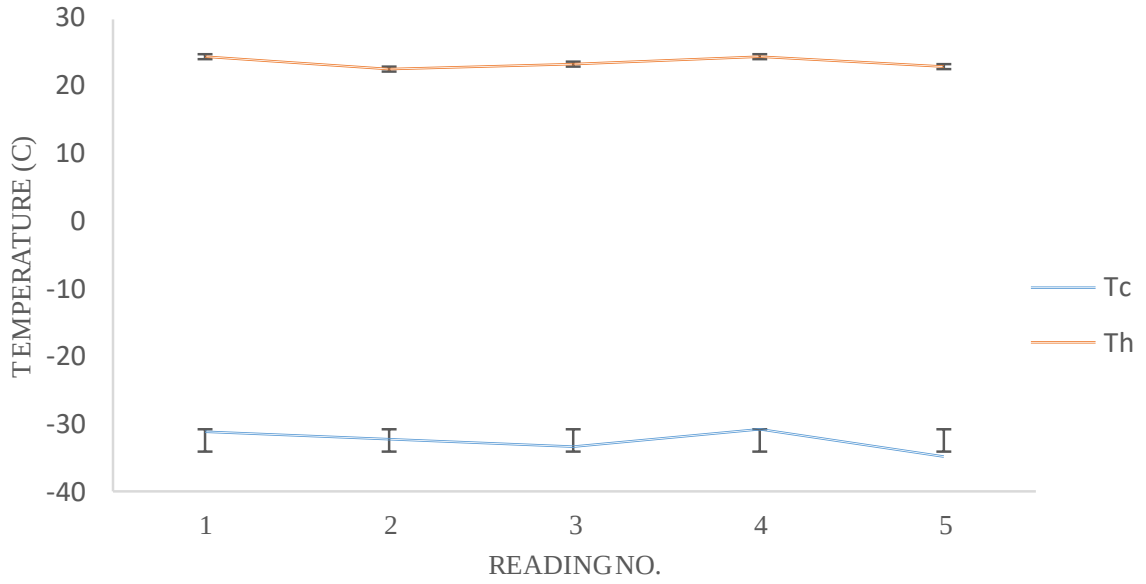

Figure A-2. Measurement uncertainty in experiment 2

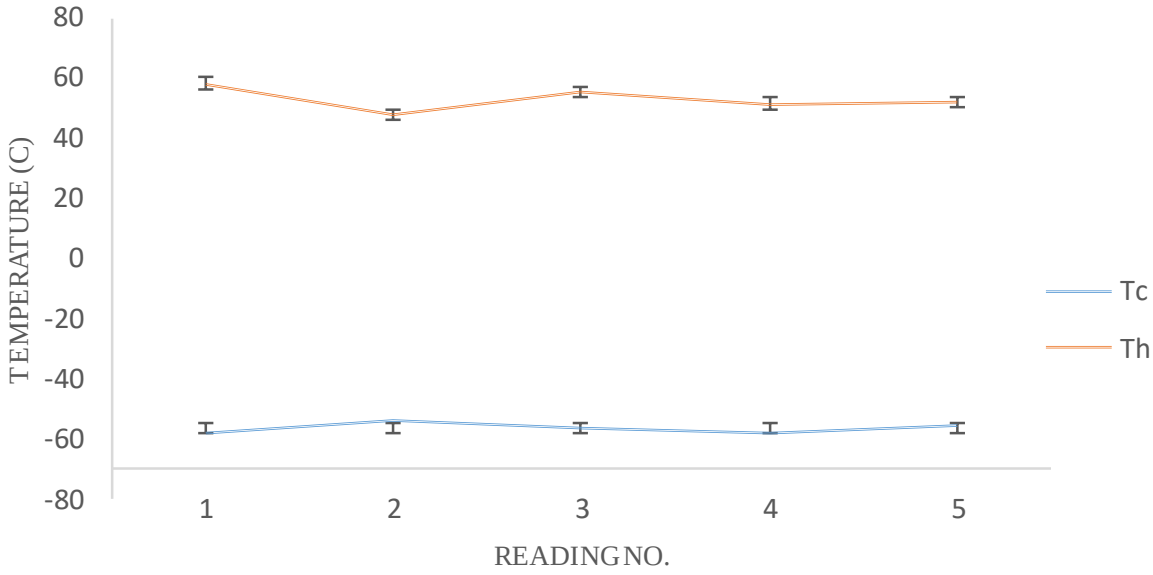

Figure A-3. Measurement uncertainty in experiment 3

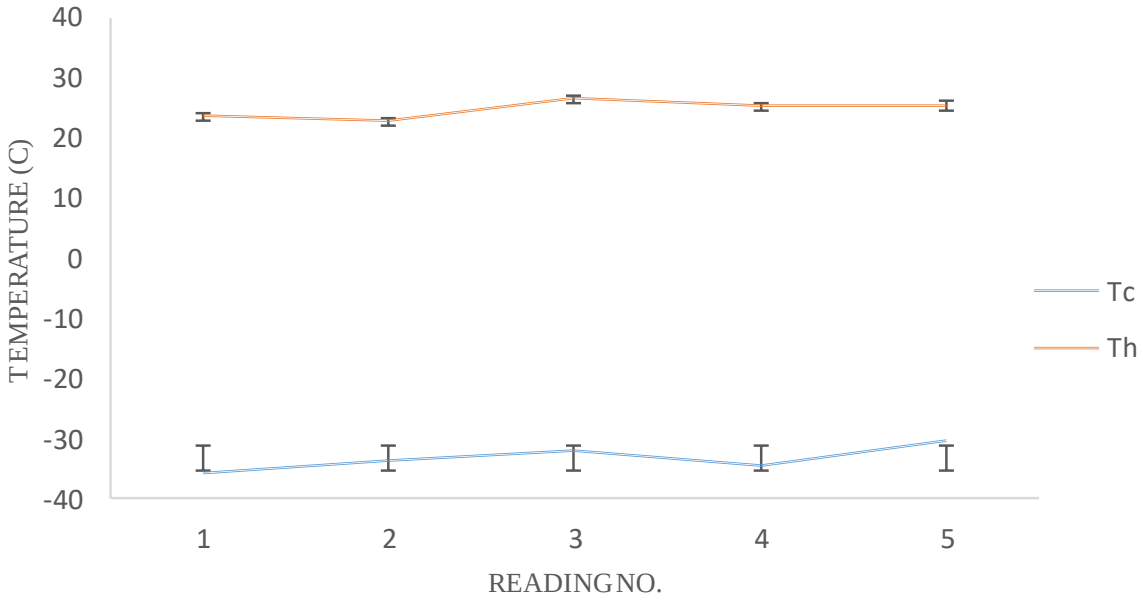

Figure A-4. Measurement uncertainty in experiment 4

Appendix B: Sensitivity Analysis

Sensitivity Analysis for the theoretical model relative to T_h (Temperature at the hot side)

The temperature at the hot side of the TEC is varied from -100% to +100% from the base value of T_h (i.e., 313.15 K) with an interval of 25% (Table B-1). All other parameters were kept constant, and the result of the analysis are presented in Figure B-1.

Table B-1. Data with the percentage change in the value of T_h

k (W/mK)	**Th (K)**	**Qc (W)**	**I (A)**	**R (Ω)**	**α** (μV/K)	**Tc (℃)**
1.6	0	2.1289	3	0.02	210	-235.707
1.6	78.2875	2.1289	3	0.02	210	-185.097
1.6	156.575	2.1289	3	0.02	210	-134.487
1.6	234.863	2.1289	3	0.02	210	-83.8767
1.6	313.15	2.1289	3	0.02	210	-33.2666
1.6	391.438	2.1289	3	0.02	210	17.34353
1.6	469.725	2.1289	3	0.02	210	67.95363
1.6	548.013	2.1289	3	0.02	210	118.5637
1.6	626.3	2.1289	3	0.02	210	169.1738

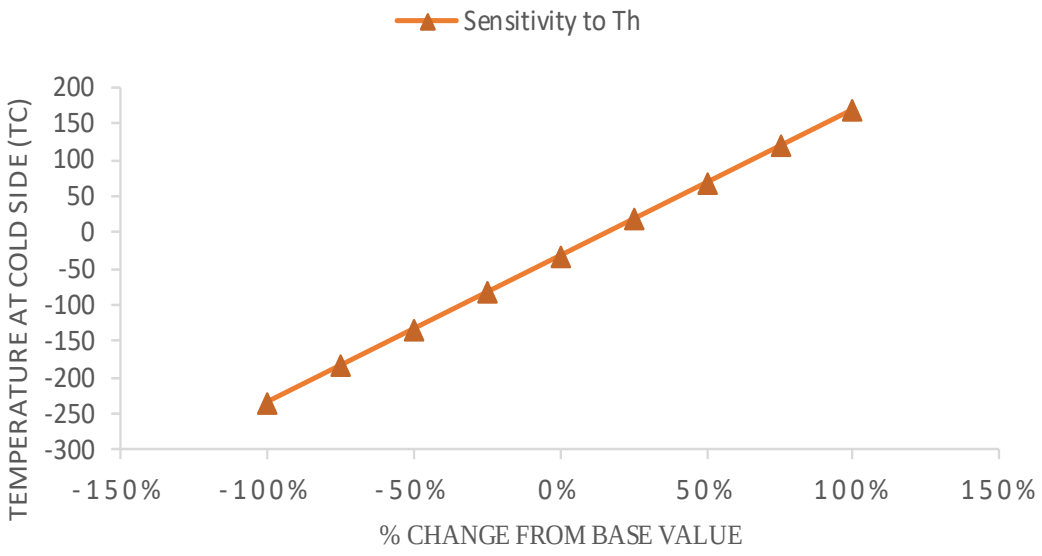

Figure B-1. The sensitivity of the theoretical model with respect to T_h

Sensitivity Analysis for the theoretical model relative to I (Current input)

The current input to the TEC is varied from -100% to +100% from the base value of I (i.e., 3 A) with an interval of 25% (Table B-2). All other parameters are kept constant, and the result of the analysis are presented in Figure B-2.

Table B-2. Data with the percentage change in the value of I

k (W/mK)	**Th (K)**	**Qc (W)**	**I (A)**	**R (Ω)**	**α** (μV/K)	**Tc (℃)**
1.6	313.15	2.13	0	0.02	210	58.86
1.6	313.15	2.13	0.75	0.02	210	21.10
1.6	313.15	2.13	1.5	0.02	210	-4.76
1.6	313.15	2.13	2.25	0.02	210	-22.13
1.6	313.15	2.13	3	0.02	210	-33.26
1.6	313.15	2.13	3.75	0.02	210	-39.70
1.6	313.15	2.13	4.5	0.02	210	-42.48
1.6	313.15	2.13	5.25	0.02	210	-42.37
1.6	313.15	2.13	6	0.02	210	-39.95

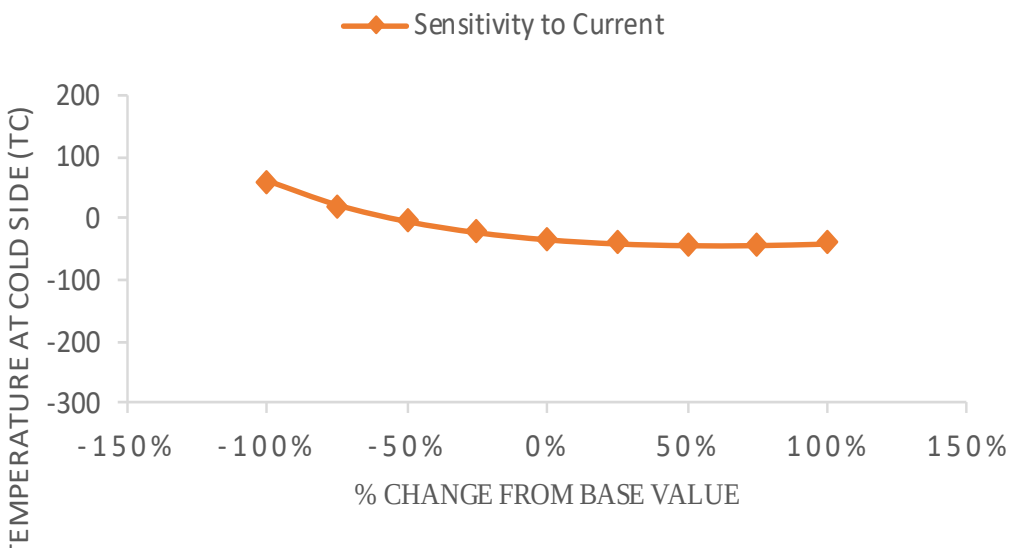

Figure B-2. The sensitivity of theoretical model with respect to current I

Sensitivity Analysis for Theoretical model relative to Q_c (Heat load)

The heat load to the TEC is varied from -100% to +100% from the base value of Q_c (i.e., 2.13 W) with an interval of 25% (Table B-3). All other parameters are kept constant, and the result of the analysis are presented in Figure B-3.

Table B-3. Data with the percentage change in the value of Q_c

k (W/mK)	**Th (K)**	**Qc (W)**	**I (A)**	**R (Ω)**	**α** (μV/K)	**Tc (℃)**
1.6	313.15	0	0	0.02	210	-45.4571
1.6	313.15	0.532225	0.75	0.02	210	-42.4094
1.6	313.15	1.06445	1.5	0.02	210	-39.3618
1.6	313.15	1.596675	2.25	0.02	210	-36.3142
1.6	313.15	2.1289	3	0.02	210	-33.2666
1.6	313.15	2.661125	3.75	0.02	210	-30.2189
1.6	313.15	3.19335	4.5	0.02	210	-27.1713
1.6	313.15	3.725575	5.25	0.02	210	-24.1237
1.6	313.15	4.2578	6	0.02	210	-21.0761

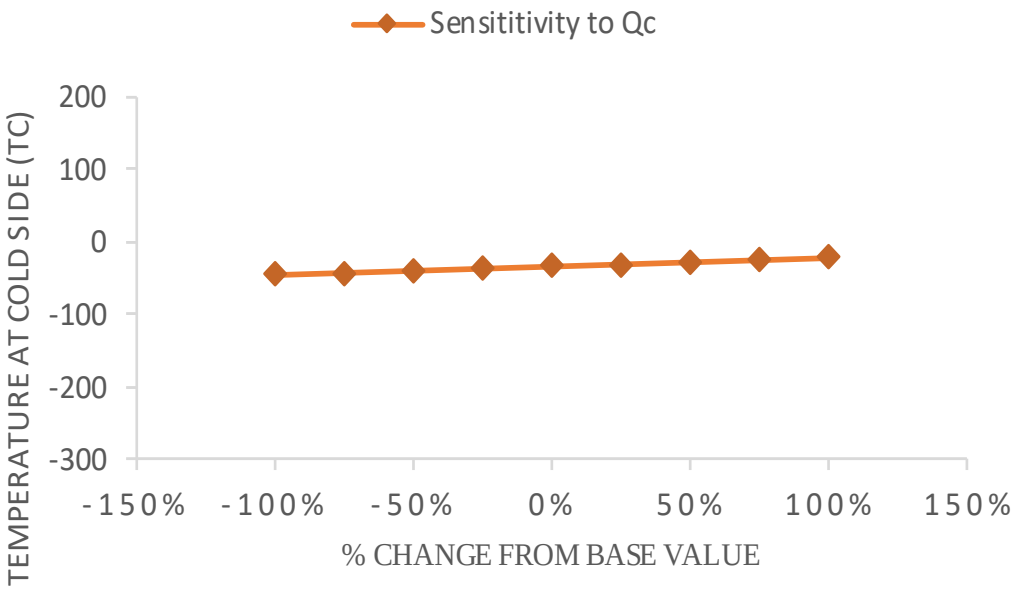

Figure B-3. The sensitivity of theoretical model with respect to heat load Q_c

Appendix C: Validation of the Simulation Tool

The stepwise design procedure in Comsol is discussed below:

1. Define geometry as in Figure C-1 using the parameters given in Table C-1.
2. Define the materials as given in Table 7-1.
3. Define the heat transfer as shown in Figure C-2, apply the boundary condition of 51℃ at the hot side. The significance of using this temperature of 51℃ lies in the fact that this simulation was performed to make a comparison with the actual experimental results. The hot side temperature of this TEC in the experiment is 51℃ (see Section 6.2).
4. Use the room temperature as the ambient temperature (T_{amb}= 300 K). This boundary condition was applied to the whole model.
5. Define the electric current in the TEC as shown in Figure C-3. The boundary condition was applied to the whole model except the ceramic plates.
6. Define Multiphysics or thermoelectricity in the semi-conductor materials as shown in Figure C-4.
7. Compute the model.

Table C-1. Geometric and operational parameters

Name of the Parameter	Value	Description
Wc	40 [mm]	Width of Ceramic Plate along x-axis
Dc	40 [mm]	Depth of Ceramic Plate along y-axis
Hc	1 [mm]	Height of Ceramic Plate along z-axis
Wcu	1.5 [mm]	Width of copper connectors along x-axis
Dcu	1.5 [mm]	Depth of copper connectors along y-axis
Hcu	.25 [mm]	Height of copper connectors along z-axis
Dte	1 [mm]	Distance between thermoelements
Wte	1.5 [mm]	Width of thermoelements along x-axis
DPte	1.5 [mm]	Depth of thermoelements along y-axis
Hte	1.5 [mm]	Height of thermoelements along z-axis
I0	5 [A]	Current input

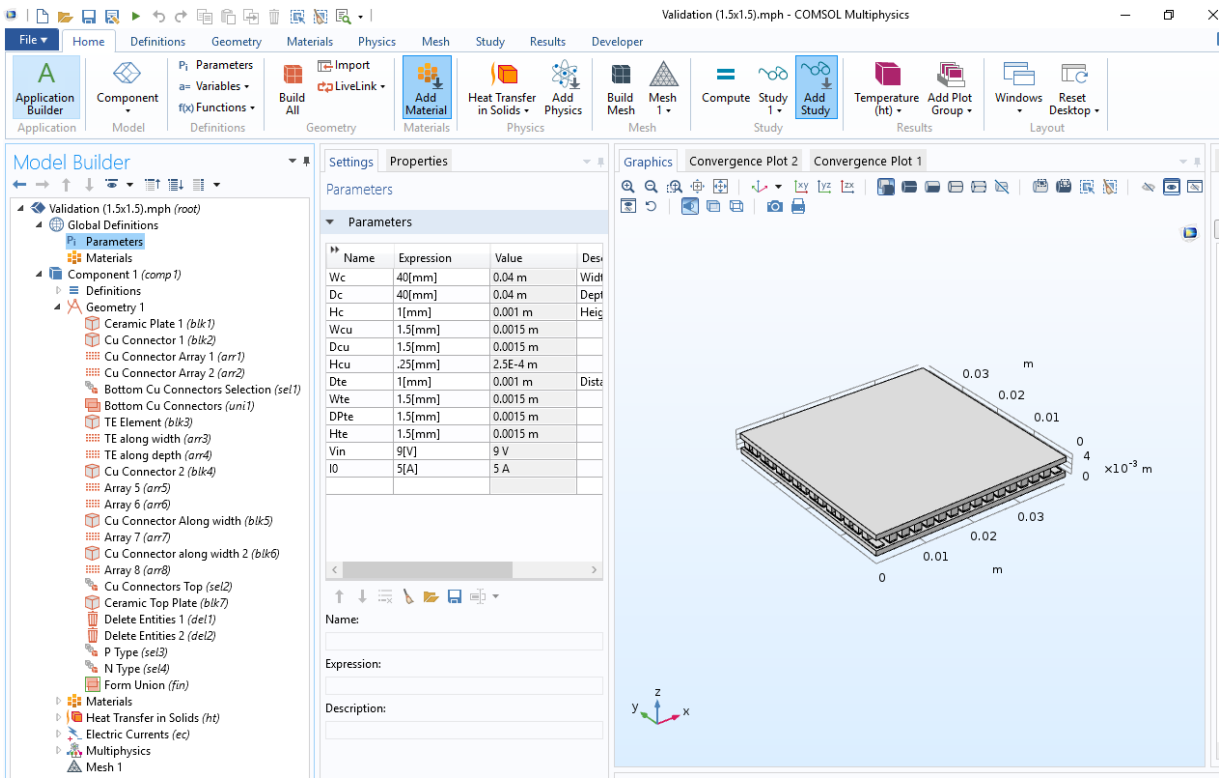

Figure C-1. Defining the geometric sequence

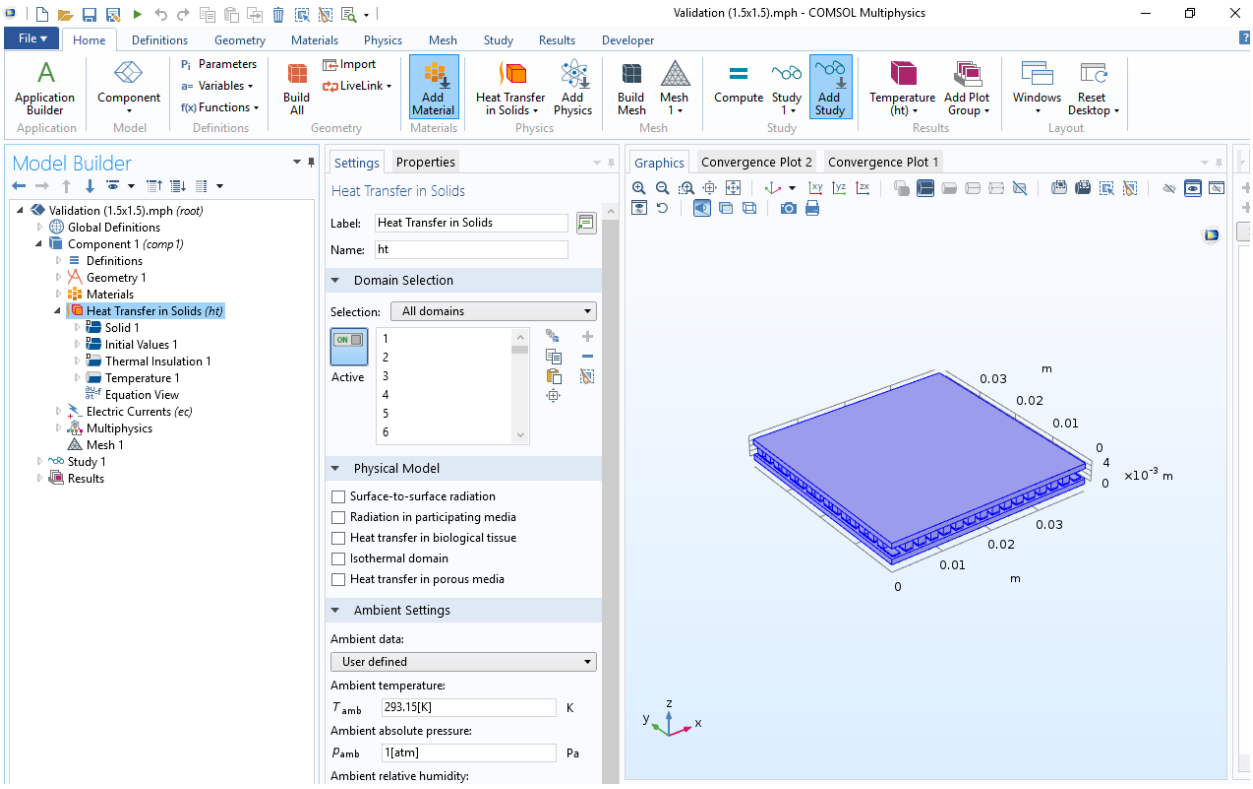

Figure C-2. Defining heat transfer physics

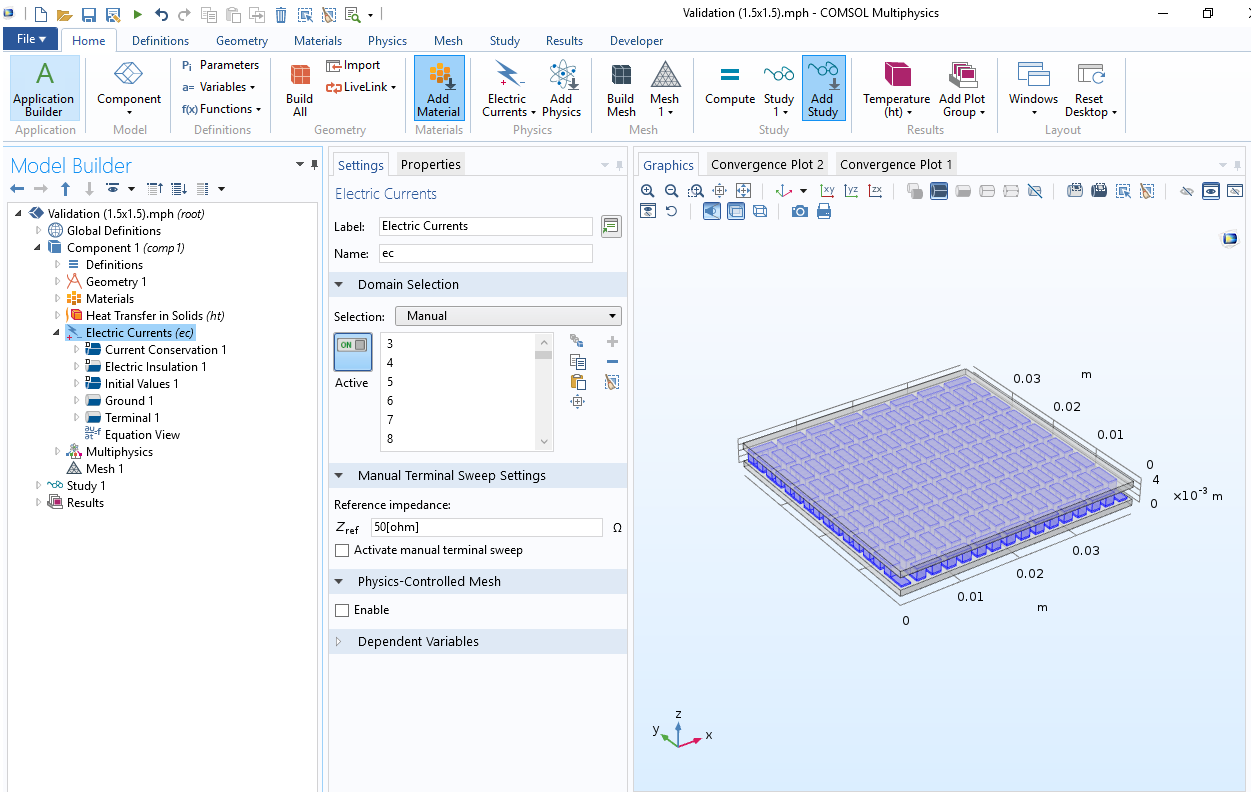

Figure C-3. Defining electric current physics

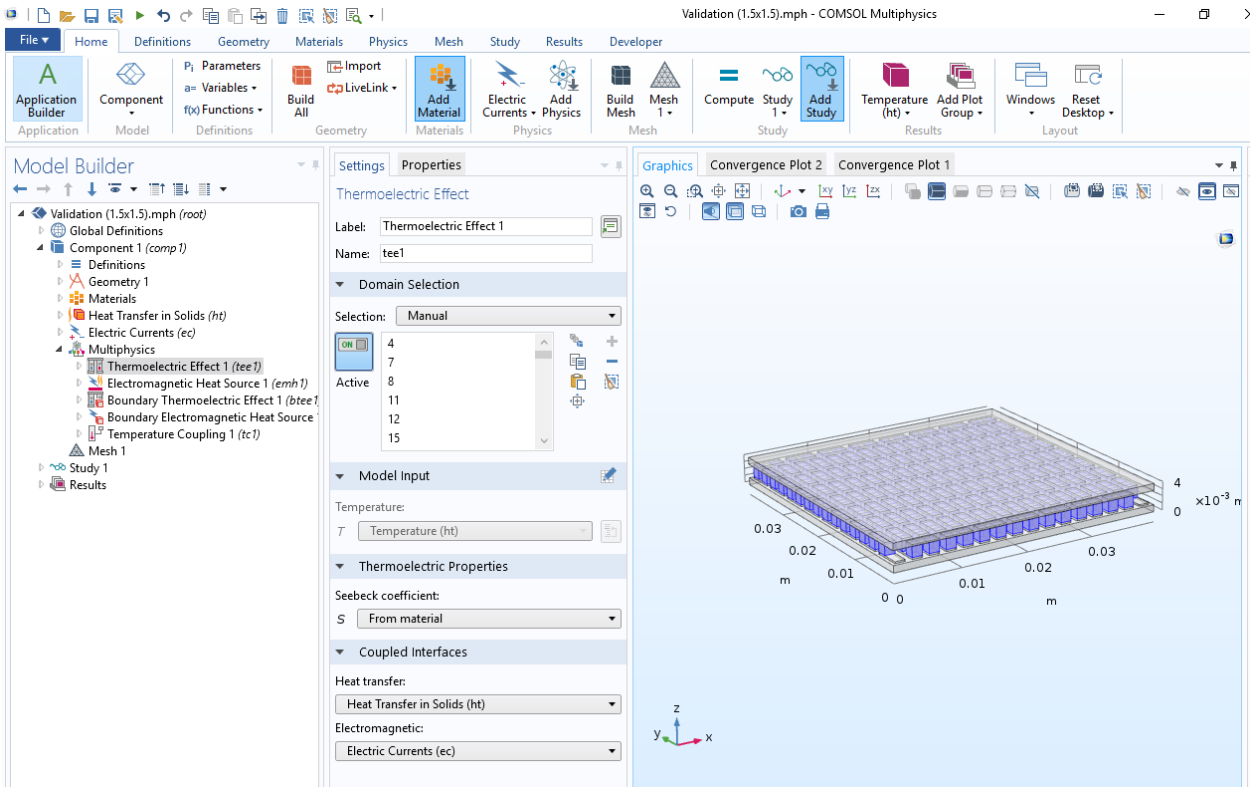

Figure C-4. Defining Multiphysics

Appendix D: Modeling of the Thermoelectric Cooler in Comsol

The stepwise design procedure is discussed below:

1. Define geometry as in Figure D-1 using the parameters given in Table D1.
2. Define materials as given in Table 7-1.
3. Define heat transfer as in Figure D-2, apply the boundary condition of 40℃ at the hot side of TEC. This was set to be 40℃ for two reasons. Firstly, the cooler was designed to give the minimum cold side temperature with the maximum hot side temperature of TEC. But for safety reasons the hot side temperature of TEC cannot be more than 45℃ as any temperature beyond this for more than 7 minutes will burn the human tissues (Yarmolenko et al., 2011). This trade-off left us with selecting the temperature of 40℃. This temperature was used as a maximum temperature limit for the pulp testing device.
4. Use the room temperature as the ambient temperature (T_{amb}= 300 K). This boundary condition was applied to the whole model.
5. Define the electric currents in the upper and lower stages separately as shown in Figure D-3. Parametrize the current between 1-8 [A] to get the optimized value of the current. This physics was applied to the whole model except the ceramic plates.
6. Define Multiphysics or thermoelectricity in the semiconductor materials as shown in Figure D-4. This only applies to thermoelectric materials.
7. Compute the model.
8. Use the application builder to build an application where any user can input parameters to study the design. The interface of the application is given in Figure D-5. This application is also included in the binary file submitted on the disk with this thesis.

Table D-1. Geometric and Operational Parameters

Stage	Name of the Parameter	Value	Description
1 (Lower stage)	Wc	22 [mm]	Width of Ceramic Plate along x-axis
	Dc	22 [mm]	Depth of Ceramic Plate along y-axis
	Hc	1 [mm]	Height of Ceramic Plate along z-axis

	Wcu	1.2 [mm]	Width of copper connectors along x-axis
	Dcu	1.2 [mm]	Depth of copper connectors along y-axis
	Hcu	.25 [mm]	Height of copper connectors along z-axis
	Dte	1 [mm]	Distance between thermoelements
	Wte	1.2 [mm]	Width of thermoelements along x-axis
	DPte	1.2 [mm]	Depth of thermoelements along y-axis
	Hte	1-8 [mm]	Height of thermoelements along z-axis
	I0	1-8 [A]	Current in stage 1
Stage 2 (Upper stage)	Wc2	11 [mm]	Width of Ceramic Plate along x-axis
	Dc2	11 [mm]	Depth of Ceramic Plate along y-axis
	Hc2	1 [mm]	Height of Ceramic Plate along z-axis
	Wcu2	1.2 [mm]	Width of copper connectors along x-axis
	Dcu2	1.2 [mm]	Depth of copper connectors along y-axis
	Hcu2	.25 [mm]	Height of copper connectors along z-axis
	Dte2	1 [mm]	Distance between thermoelements
	Wte2	1.2 [mm]	Width of thermoelements along x-axis
	DPte2	1.2 [mm]	Depth of thermoelements along y-axis
	Hte2	1-4 [mm]	Height of thermoelements along z-axis
	I02	1-8 [A]	Current in stage 2

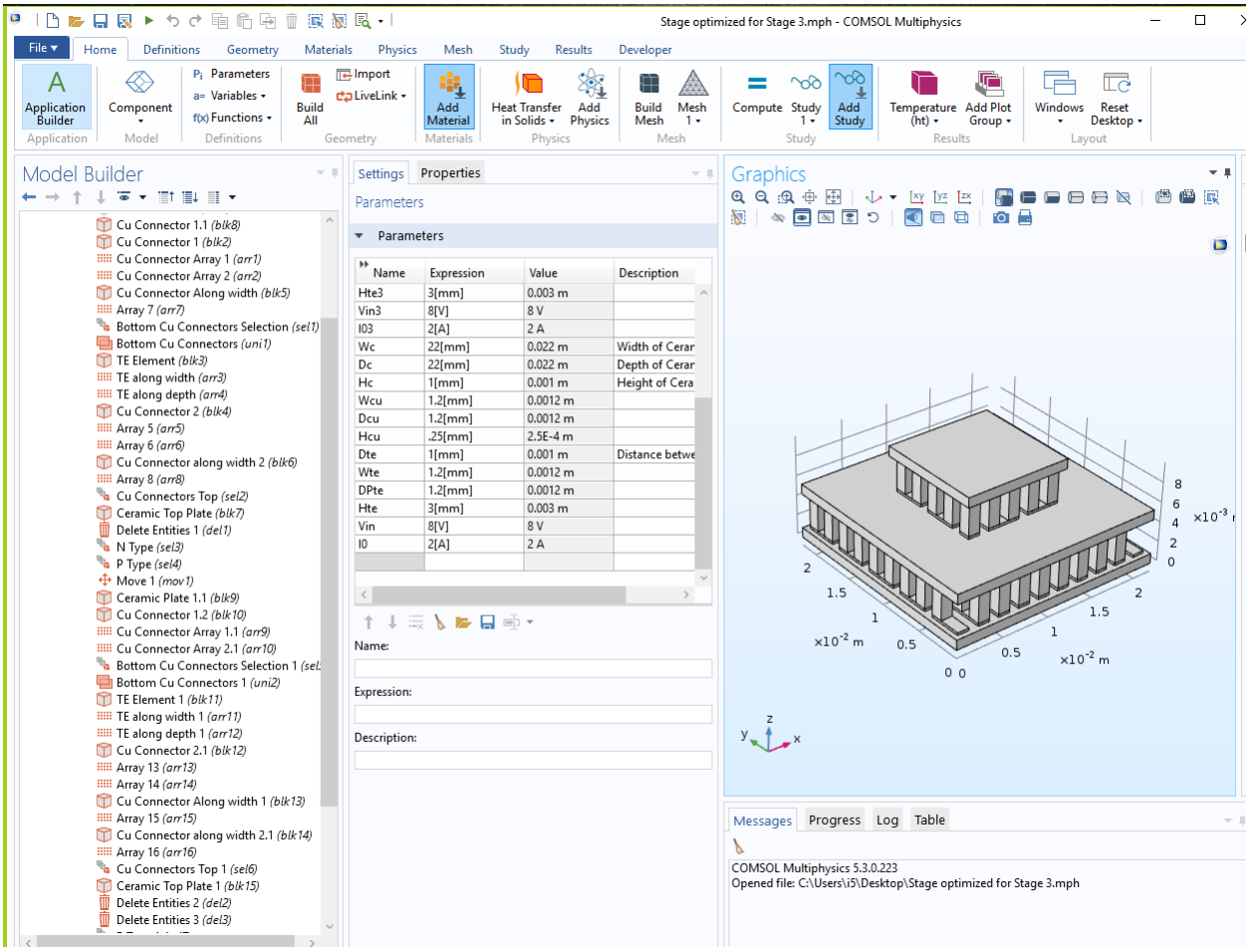

Figure D-1. Defining the geometric sequence

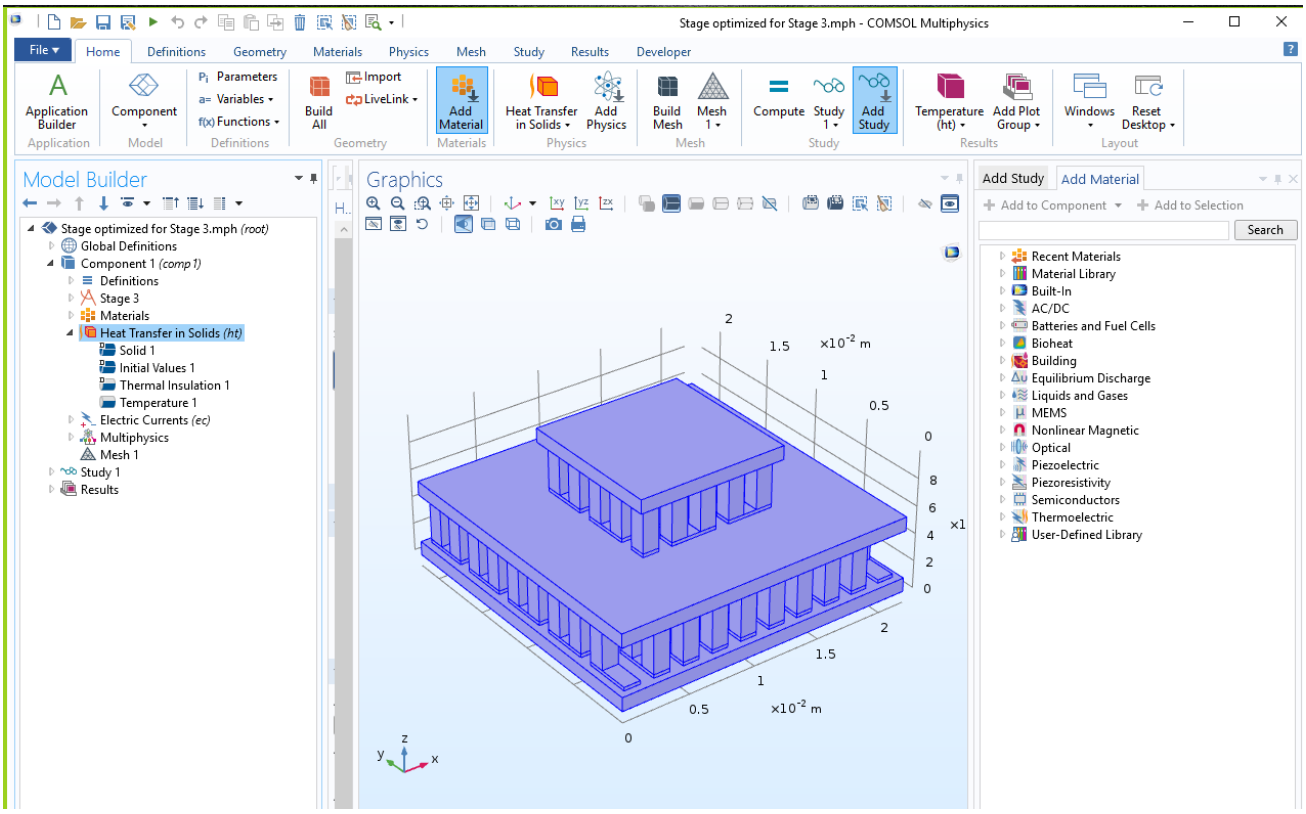

Figure D-2. Defining heat transfer physics

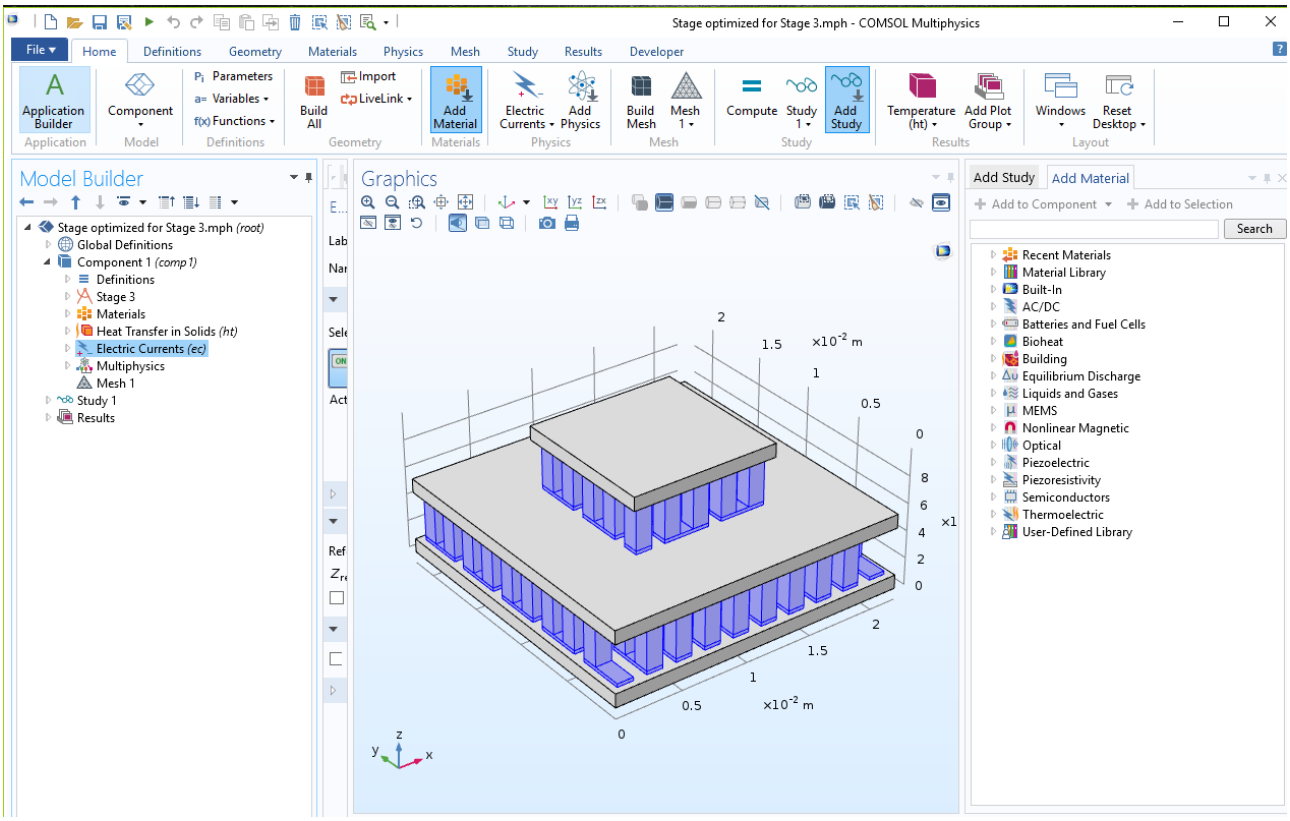

Figure D-3. Defining electric current physics

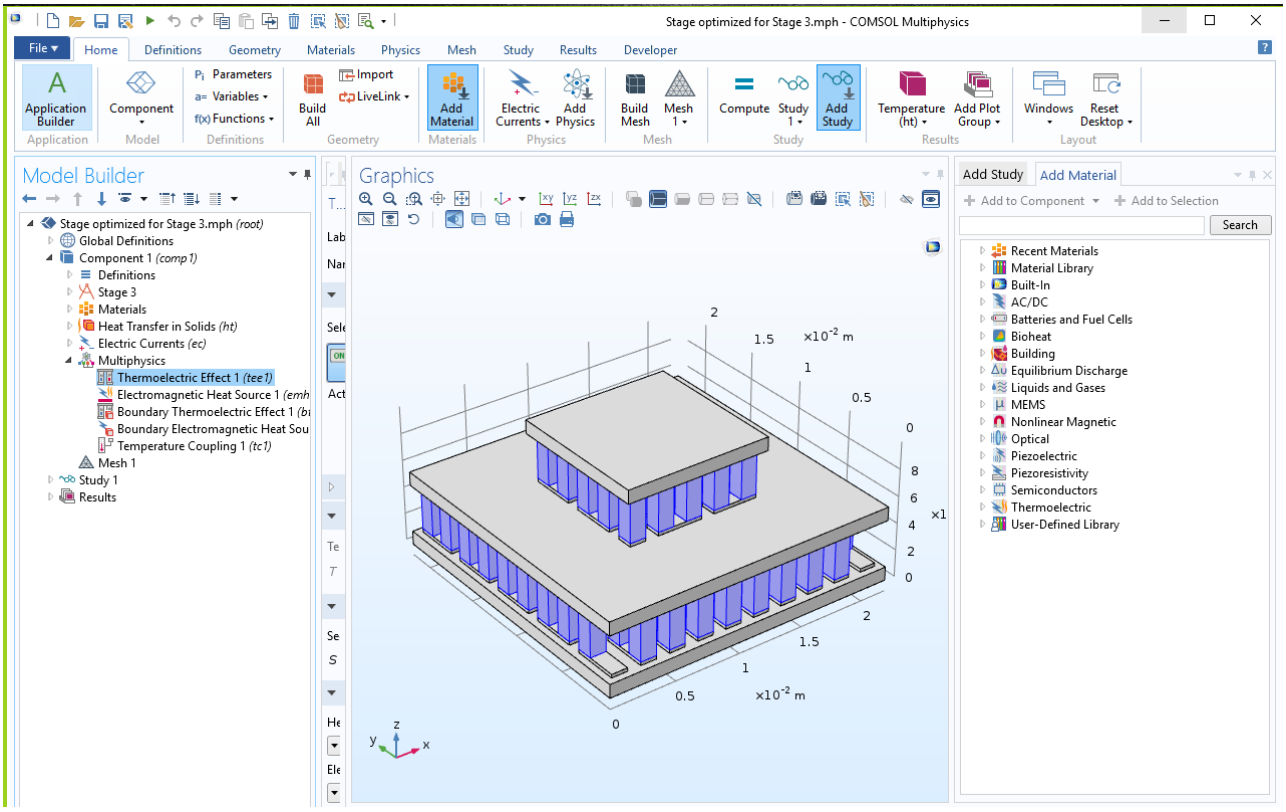

Figure D-4. Defining Multiphysics

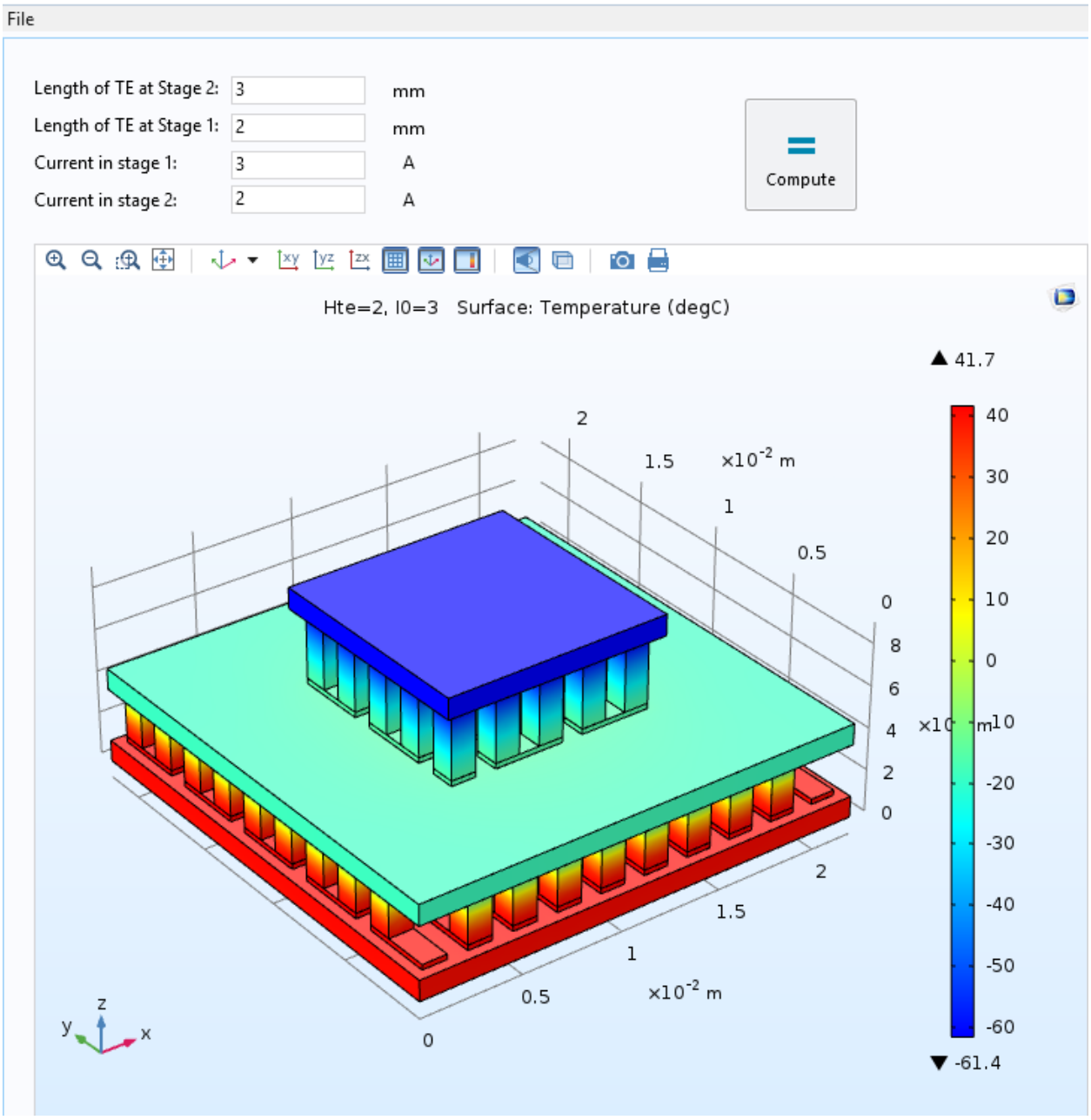

Figure D-5. Application Interface

Appendix E: Modeling of the Vapor Chamber

For the vapor chamber, the flat heat pipe model of Comsol was utilized (Comsol version 5.2a, 2016). This model was then modified to the following dimensions given in Table E-1 as per the requirement of the design and the material was changed from copper to aluminum.

Table E-1. Geometric Parameters used for the Vapor Chamber

Parameter	Expression	Description
Length	60, 80 [mm]	Length of VC
Width	30 [mm]	Width of VC
Height	5 [mm]	Height of VC
d_wall	.75 [mm]	Wall thickness
d_wick	1 [mm]	Wick thickness
Q_{in}	30 [W]	Heat load

Appendix F: Permission to Reproduce the Figure(S) in Literature

JOHN WILEY AND SONS LICENSE TERMS AND CONDITIONS

Apr 26, 2018

This Agreement between Mr. Bilal Mustafa ("You") and John Wiley and Sons ("John Wiley and Sons") consists of your license details and the terms and conditions provided by John Wiley and Sons and Copyright Clearance Center.

License Number	4310320649853
License date	Mar 15, 2018
Licensed Content Publisher	John Wiley and Sons
Licensed Content Publication	Wiley oBooks
Licensed Content Title	Thermoelectrics
Licensed Content Author	HoSung Lee
Licensed Content Date	Oct 26, 2010
Licensed Content Pages	80
Type of use	Dissertation/Thesis
Requestor type	University/Academic
Format	Print and electronic
Portion	Figure/table
Number of figures/tables	1
Original Wiley figure/table number(s)	Performance Charts from Chapter 3
Will you be translating?	No
Title of your thesis / dissertation	DESIGN OF A NOVEL THERMO-ELECTRIC COOLING DEVICE CAPABLE OF ACHIEVING CRYOGENIC TEMPERATURES FOR DENTAL PULP TESTING
Expected completion date	Apr 2018
Expected size (number of pages)	87
Requestor Location	Mr. Bilal Mustafa 215 Atton Court Saskatoon, SK s7w 0k8 Canada Attn: Mr. Bilal Mustafa
Publisher Tax ID	EU826007151